Gondwana Research xxx (2015) xxx–xxx

Contents lists available at ScienceDirect

Gondwana Research

journal homepage: www.elsevier.com/locate/gr

Global climate perturbations during the Permo-Triassic mass extinctions recorded by continental tetrapods from South Africa

Kévin Rey [a,*], Romain Amiot [a], François Fourel [a], Thomas Rigaudier [b], Fernando Abdala [c], Michael O. Day [c], Vincent Fernandez [c,d], Frédéric Fluteau [e], Christian France-Lanord [b], Bruce S. Rubidge [c], Roger M. Smith [c,f], Pia A. Viglietti [c], Bernhard Zipfel [c], Christophe Lécuyer [a,1]

[a] CNRS UMR 5276, Université Claude Bernard Lyon 1 and Ecole Normale Supérieure de Lyon, 2, Rue Raphaël Dubois, 69622 Villeurbanne Cedex, France
[b] Centre de Recherches Pétrologiques et Géochimiques (CRPG), UMR CNRS 7358, Vandoeuvre les Nancy 54501 France
[c] Evolutionary Studies Institute, School of Geosciences, University of the Witwatersrand, P. Bag 3, WITS 2050, Johannesburg, South Africa
[d] European Synchrotron Radiation Facility (ESRF), Grenoble, France
[e] Institut de Physique du Globe de Paris, 2 place Jussieu, F-75005 Paris, France
[f] Iziko South African Museum of Cape Town, P.O. Box 61, Cape Town, 8000, South Africa

ARTICLE INFO

Article history:
Received 29 July 2015
Received in revised form 14 September 2015
Accepted 15 September 2015
Available online xxxx

Handling Editor: I.D. Somerville

Keywords:
Permo-Triassic
Paleoclimate
Stable isotopes
Vertebrate apatite
Karoo Basin

ABSTRACT

Several studies of the marine sedimentary record have documented the evolution of global climate during the Permo-Triassic mass extinction. By contrast, the continental records have been less exploited due to the scarcity of continuous sections from the latest Permian into the Early Triassic. The South African Karoo Basin exposes one of the most continuous geological successions of this time interval, thus offering the possibility to reconstruct climate variations in southern Laurasia from the Middle Permian to Middle Triassic interval. Both air temperature and humidity variations were estimated using stable oxygen ($\delta^{18}O_p$) and carbon ($\delta^{13}C_c$) isotope compositions of vertebrate apatite. Significant fluctuations in both $\delta^{18}O_p$ and $\delta^{13}C_c$ values mimic those of marine records and suggest that stable isotope compositions recorded in vertebrate apatite reflect global climate evolution. In terms of air temperature, oxygen isotopes show an abrupt increase of about +8 °C toward the end of the Wuchiapingian. This occurred during a slight cooling trend from the Capitanian to the Permo-Triassic boundary (PTB). At the end of the Permian, an intense and fast warming of +16 °C occurred and kept increasing during the Olenekian. These thermal fluctuations may be related to the Emeishan (South China) and Siberian volcanic paroxysms that took place at the end of the Capitanian and at the end of the Permian, respectively. Vertebrate apatite $\delta^{13}C_c$ partly reflects the important fluctuations of the atmospheric $\delta^{13}C$ values, the differences with marine curves being likely due to the evolution of local humidity. Both the oxygen and carbon isotope compositions indicate that the PTB was followed by a warm and arid phase that lasted 6 Ma before temperatures decreased, during the Late Anisian, toward that of the end-Permian. Environmental fluctuations occurring around the PTB that affected both continental and marine realms with similar magnitude likely originated from volcanism and methane release.

1. Introduction

The End-Permian mass extinction is repeatedly shown to be the largest and most devastating, with estimates varying between 57–83% of marine genera (Raup and Sepkoski, 1982; Erwin, 1993; Sepkoski, 1996; Bambach et al., 2002; Alroy, 2008, 2010; McGhee et al., 2013) and 70% of continental tetrapod families (Maxwell, 1992), with extinctions in both realms appearing in several cases to occur in pulses (Song et al., 2013; Smith and Botha-Brink, 2014) over a total duration of 96 thousand to several hundred thousand years (Mundil et al., 2004; Huang et al., 2011, 2012; Smith and Botha-Brink, 2014). Plant species also suffered from this event with, for example, the extinction of the seed fern *Glossopteris* replaced by a *Dicroidium*-dominated flora (McLoughlin et al., 1997).

The causes of the end-Permian mass extinction event have been widely discussed. Most authors agree on climatic deterioration due to the release of several gasses into the atmosphere by volcanic activity that formed the Siberian Traps (Retallack and Jahren, 2008; Grasby et al., 2011; Sobolev et al., 2011; Sanei et al., 2012). Several authors suggested concomitant events such as a significant release of methane from both permafrost and marine clathrates (De Wit et al., 2002; Heydari and Hassanzadeh, 2003; Ryskin, 2003; Retallack et al., 2003) or from coal-

* Corresponding author at: CNRS UMR 5276, Université Claude Bernard Lyon 1 and Ecole Normale Supérieure de Lyon, 2, Rue Raphaël Dubois, 69622 Villeurbanne Cedex, France.
E-mail address: kevin.rey@univ-lyon1.fr (K. Rey).
[1] Also at Institut Universitaire de France.

http://dx.doi.org/10.1016/j.gr.2015.09.008
1342-937X/

bed cross-cut by igneous intrusions (McElwain et al., 2005; Retallack et al., 2006; Retallack and Jahren, 2008). Using stable carbon isotope compositions of paleosol carbonate nodules, Ward et al. (2005) interpreted the Permo-Triassic crisis as a progressive environmental degradation rather than an instantaneous event. In the oceans, large sustained anoxia has been reported and is considered to have at least partly triggered the marine extinction (Isozaki, 1997; Nielsen and Shen, 2004; Algeo et al., 2011; Dustira et al., 2013). The evidence from geographically disparate areas and diverse environments is highly supportive of global warming (Benton and Newell, 2014).

Another mass extinction occurring at the Guadalupian–Lopingian Boundary (GLB), about 10 Ma before the Permo-Triassic Boundary (PTB), has been identified (Stanley and Yang, 1994). The intensity and duration of this extinction event is uncertain, some authors ranking it alongside the five major Phanerozoic mass extinction events (Stanley and Yang, 1994; Bond et al., 2010) whereas others only considered it as a low diversity point (Yang et al., 2000; Clapham et al., 2009; Groves and Wang, 2013). During the GLB, several species became extinct whether they lived at low or high latitudes (Bond et al., 2015) either in oceans or continents (Bond et al., 2010). On continents, the extinction affected plants with some turnover in South China (Bond et al., 2010), in South Africa, and in Antarctica (Retallack et al., 2006) and eventually a few vertebrate species with the extinction of the dinocephalian tetrapods (Retallack et al., 2006; Sahney and Benton, 2008; Day, 2013; Day et al., 2015). Several causes have been reported to explain these extinctions, including the Emeishan basalt flood in South China (Sephton et al., 2002; Zhou et al., 2002; Wignall et al., 2009), marine anoxia (Weidlich, 2002; Detian et al., 2013; Saitoh et al., 2013), methane outburst (Retallack et al., 2006; Retallack and Jahren, 2008) or even global marine regression (Jin et al., 1994; Hallam and Wignall, 1999; Yue and Yugan, 2000; Saitoh et al., 2013).

This study aims to investigate the climatic perturbations of these two events through the analysis of stable oxygen and carbon isotope compositions of continental vertebrate apatite. The oxygen isotope composition ($\delta^{18}O$) of vertebrate apatite (bone, teeth) reflects both the $\delta^{18}O_{bw}$ value of the animal body water and its body temperature. For most terrestrial vertebrates, the ingested oxygen comes from drinking meteoric water or plant water, (D'Angela and Longinelli, 1990; Kohn et al., 1996). The oxygen isotope composition of meteoric water ($\delta^{18}O_{mw}$) depends on climatic parameters such as air temperature, hygrometry, and amount of precipitation (Dansgaard, 1964; Grafenstein et al., 1996; Fricke and O'Neil, 1999), thus vertebrates indirectly record the climatic conditions of their environment in their phosphatic tissues. It is noted, however, that the $\delta^{18}O_w$ value of surface waters can differ from that of precipitation as a result of local earth surface processes such as evaporation, addition of soluble dust, and mixing with other water sources, thus complicating the interpretations in terms of climatic reconstructions. Using empirically derived phosphate–water oxygen isotope fractionation equations, it is thus possible to estimate the $\delta^{18}O_{mw}$ value, and related local mean air temperatures (T_{air}) provided that the ancient $\delta^{18}O_{mw}$–T_{air} relationship did not differ significantly from that of the present-day. The carbon isotope composition ($\delta^{13}C_c$) of vertebrate apatite mainly reflects that of the animal's diet with ^{13}C-enrichments varying among animals, being most likely as a result of different digestive physiologies (DeNiro and Epstein, 1978; Quade et al., 1992; Passey et al., 2005). Herbivorous animals have apatite $\delta^{13}C_c$ values reflecting that of their herbivorous diet, whereas carnivorous forms have carbon isotope compositions reflecting the $\delta^{13}C$ value of the flesh of their prey. The prey tissue itself reflects the $\delta^{13}C$ value of their plant diet with a flesh-plant ^{13}C-enrichment of about $1 \pm 1‰$ (Barnes et al., 2007). In turn, plants have carbon isotope compositions mainly controlled by their photosynthetic pathway (see Ehleringer and Monson (1993) for a review).

The C_3 pathway is the most common, occurring in all trees, most shrubs and herbs, and grasses in regions with a cool growing season. Today, C_3 plants have a mean $\delta^{13}C$ value of −27‰ (range from −35‰ to −22‰). Abiotic factors indirectly influence the carbon isotope compositions of C_3 plants by affecting leaf stomatal conductance, which in turn constrains the amount of CO_2 diffusion through plant epidermis. Variations in sunlight intensity, water volume and osmotic stress, local temperature and pCO_2 produce variations in the $\delta^{13}C$ values of C_3 plants (reviewed in Ehleringer and Monson, 1993).

Therefore, variations in $\delta^{13}C_c$ values in vertebrate apatite reflect both variations in atmospheric $\delta^{13}C$ values and that of local humidity. C_4 photosynthesis operates in grasses from regions with a warm growing season, and in some sedges and dicotyledons. Finally, crassulacean acid metabolism (CAM) occurs in succulent plants. Because C_4 and CAM plants only appeared during the Cenozoic and were apparently absent in Permian and Triassic ecosystems, they are not considered relevant to this study.

The Main Karoo Basin of South Africa records both the Capitanian and end-Permian extinction events within a single near-continuous sequence. We analyzed tetrapod tooth apatite from tetrapod fossils from the Beaufort Group, spanning five Permian and four Triassic biozones (Hancox et al., 1995; Rubidge, 1995; Shishkin et al., 1995; Neveling et al., 2005; Rubidge, 2005). The rocks of the Beaufort Group, the earliest non-marine sequence in the Karoo retroarc foreland system (Catuneanu et al., 1998; Smith and Ward, 2001; De Kock and Kirschvink, 2004; Ward et al., 2005; Botha and Smith, 2007; Coney et al., 2007; Fildani et al., 2009; Botha-Brink et al., 2014), preserve an uninterrupted record from the Middle Permian to the Middle Triassic (Ochev and Shishkin, 1989; Hancox et al., 1995; Rubidge, 1995; Hancox and Rubidge, 1996). They were deposited mainly under fluvial, but also lacustrine conditions, under a semi-arid climate (Smith et al., 1993; Smith, 1995; Rubidge et al., 2000; Retallack et al., 2003). A diverse vertebrate fauna that includes therapsids, amphibians, archosauromorphs and parareptiles, has been recovered from this sedimentary succession and the bones of some of these were sampled for geochemical studies.

In this study, apatite from the bones and teeth of therapsids, erythrosuchids, pareiasaurids and temnospondyls were analyzed for their oxygen and carbon isotope compositions, which are interpreted as proxy for atmospheric temperature variations, as well as relative humidity. Results were compared to marine carbonate $\delta^{13}C$ curves in order to distinguish between the local changes in Karoo Basin environments (arid or humid) from the global trends (temperature, pCO_2) and also to discuss the factors that triggered these changes.

2. Material and methods

2.1. Sampling

A total of 39 teeth and 97 bones were sampled from 116 fossil individuals and analyzed for the stable oxygen isotope composition of phosphate group, oxygen and carbon isotope compositions of carbonate group and carbonate content in apatite. Sampled specimens from the collections of Iziko South African Museum in Cape Town and the Evolutionary Studies Institute, University of the Witwatersrand comprise Therapsida, Archosauromorpha, Pareiasauridae and Temnospondyli recovered from 17 farm localities (Fig. 1). Fossil samples from each locality are attributed to one of nine biozones (supplementary material; Rubidge, 2005), for which radiometric dates provide absolute temporal constraints (Rubidge et al., 2013; Day et al., 2015). More information on locality attribution to their biozones are provided in supplementary material.

Calculation of paleogeographic coordinates of the sampling sites was made using the Apparent Polar Wander Path of Gondwana (Torsvik et al., 2012). This APWP was constructed using a selection of the best paleomagnetic poles available calculated on a 10 Ma window. Paleolatitudes and associated uncertainties are shown in

Please cite this article as: Rey, K., et al., Global climate perturbations during the Permo-Triassic mass extinctions recorded by continental tetrapods from South Africa, Gondwana Research (2015), http://dx.doi.org/10.1016/j.gr.2015.09.008

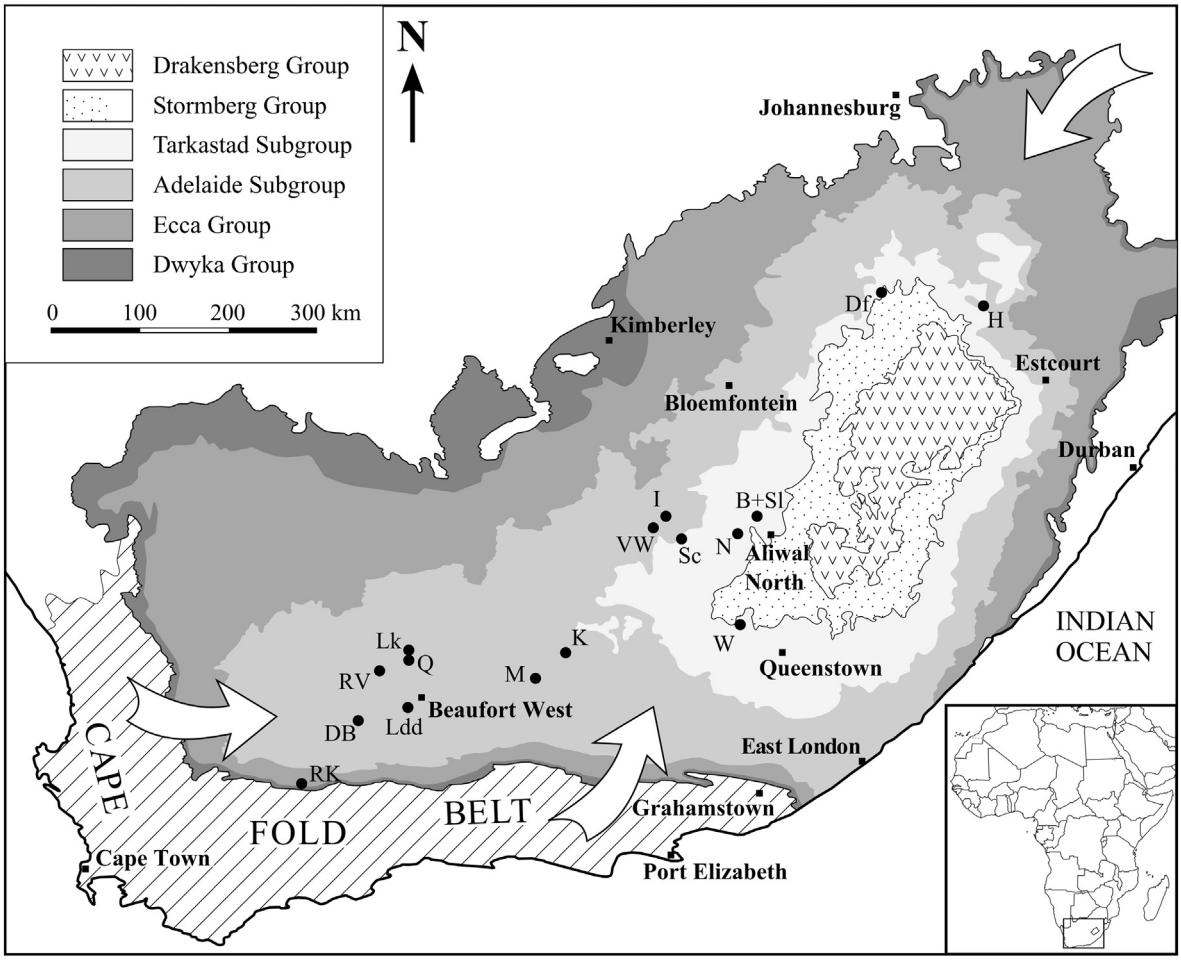

Fig. 1. Distribution map of studied Permian and Triassic tetrapod-bearing localities reported along with the main lithostratigraphic units of the Main Karoo Basin bordering with the Cape Fold Belt. The white arrows illustrate the possible sediment origins and water supplies of the three areas. B: Bethel; DB: Die Bad; Df: Driefontein; H: Harrismith Commonage; I: Inhoek; K: Klipfontein; Ldd: La-de-da; Lk: Leuuw Kloof; M: Matjeshoek; N: Nooitgedacht; Q: Quaggafontein; RK: Ruiters Kop; RV: Ryers Valley; Sc: Schalkwykskraal; Sl: Slootkraal; VW: Van Wyksfontein; W: Wilgerkloof.

supplementary material. These uncertainties depend on the quality and number of magnetic poles used to build the APWP.

2.2. Stratigraphic correlations

All sampled localities have been positioned within a stratigraphic and geochronological framework (Fig. 2) and correlated to the marine stages using the absolute ages accepted by the International Commission on Stratigraphy (Cohen et al., 2013), with the exceptions of the Permo-Triassic and Guadalupian–Lopingian boundaries considered to be 251.90 ± 0.02 Ma and 259.1 ± 0.5 Ma in age as calculated by Burgess et al. (2014) and Zhong et al. (2014), respectively. Permian biozone ages are taken from Day et al. (2015). The end of the *Dicynodon* AZ is characterized by the last appearance datum (LAD) of *Dicynodon* and *Daptocephalus* (see van der Walt et al., 2010), which is correlated with the PTB in the lower part of the Palingkloof Member (Smith, 1995, Ward et al., 2005)). As absolute dates have not yet been determined for the rocks of the Triassic middle and upper Beaufort, age determination has been achieved by biostratigraphic correlation with Laurasian sequences (see Hancox et al., 1995; Rubidge, 2005; Abdala and Ribeiro, 2010).

2.3. Analytical techniques

To measure the oxygen isotope composition of the apatite phosphate group, we used acid dissolution and anion-exchange resin to isolate the phosphate ions according to a protocol derived from the original method published by Crowson et al. (1991) and slightly modified by Lécuyer et al. (1993). Silver phosphate was quantitatively precipitated in a thermostatic bath set at a temperature of 70 °C. After filtration, washing with double deionized water, and drying at 50 °C, an aliquot of 300 μg of Ag_3PO_4 was mixed with 300 μg of nickelized carbon in a silver reaction capsule. Silver phosphate was then reduced into CO to measure its $^{18}O/^{16}O$ ratio according to the protocol developed by Lécuyer et al. (2007) and Fourel et al. (2011). Each sample was heated at 1450 °C by pyrolysis using a VarioPYROcube EA system (Elementar™) interfaced to an IsoPrime isotope ratio mass spectrometer working in continuous flow mode at the UMR CNRS 5276 LGLTPE, University Claude Bernard Lyon 1. Isotopic compositions are quoted in the standard δ notation relative to V-SMOW. Silver phosphate precipitated from standard NBS120c (natural Miocene phosphorite from Florida) was repeatedly analyzed ($\delta^{18}O = 21.66 \pm 0.22‰$; n = 25) along with the silver phosphate samples derived from the tetrapod remains. For the oxygen and carbon isotope analysis of apatite carbonate, about 10 mg of enamel, dentine or bone powder was pre-treated according to the procedure of Koch et al. (1997). Powders were washed with a 2% NaOCl solution to remove organic matter. Powders were then rinsed five times with double deionized water and air-dried at 40 °C during 24 h. 0.1 M Acetic acid was then added to remove potential secondary carbonate. After 24 h of acid digestion, the powder was rinsed again five times with double deionized water and air-dried at 40 °C during 24 h. The powder/solution ratio was kept constant at 0.04 g mL^{-1} for

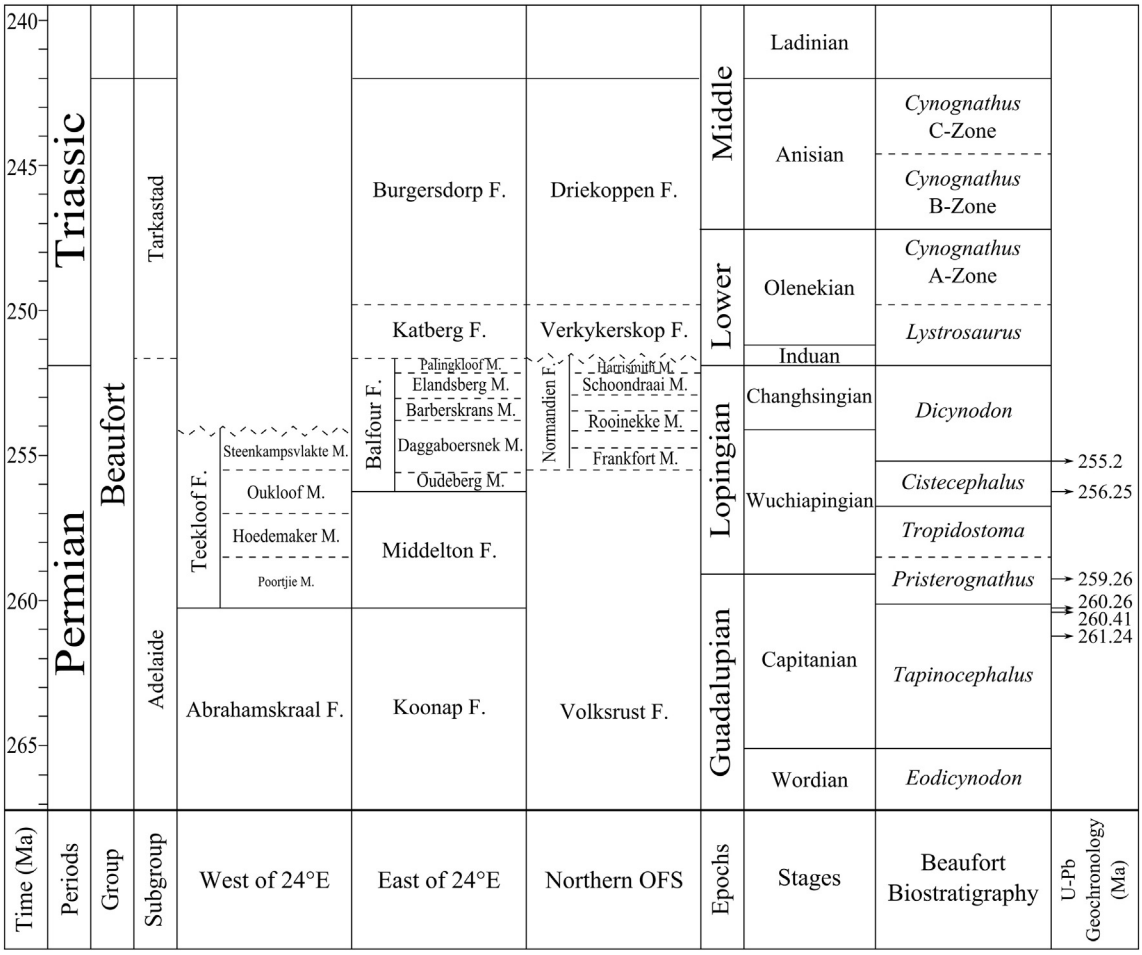

Fig. 2. Integrated stratigraphic chart of the Main Karoo Basin and tentatively correlated to the Assemblage zones and the marine stages based on Hancox et al. (1995), Rubidge (2005), Abdala and Ribeiro (2010), Rubidge et al. (2013) and Day et al. 2015. Boundaries without absolute ages are represented with dashed lines. F.: Formation; M.: Member.

both treatments. Stable isotope ratios were determined by using an auto sampler Gasbench coupled to a Thermo Scientific MAT253 isotope ratio mass spectrometer (IRMS) at the CRPG UMR 7358 CNRS-UL, Vandoeuvre les Nancy. For each sample, an aliquot between 2 and 4 mg of pre-treated apatite was reacted with 2 mL of supersaturated orthophosphoric acid at 70 °C for at least 5 h under a He atmosphere before starting 10 measurement cycles of the isotopic composition of the produced CO_2 with a Finnigan MAT 253 continuous flow isotope ratio mass spectrometer. Isotopic compositions are quoted in the delta notation in ‰ relative to V-PDB for carbon and converted to V-SMOW for oxygen. All sample measurements were adjusted to the internal reference calibrated on the international standards IAEA CO-1, IAEA CO-8 and NBS 19.

3. Results

For each sample, the isotopic composition of oxygen, phosphate ($\delta^{18}O_p$) and carbonate ($\delta^{18}O_c$), and carbon ($\delta^{13}C_c$), as well as the carbonate content in weight percent are reported in supplementary material. The $\delta^{18}O_p$ values of all tetrapods range from −0.5‰ to +13.6‰ V-SMOW. After discarding values corresponding to samples that were likely affected by diagenetic alteration (see Discussion section), as well as one outlier (sample SA50) having both oxygen and carbon isotope compositions significantly different (at 95% confidence interval) than other samples from the same age, the remaining values were plotted against their age as bulk values in Fig. 3 and averages of the four represented taxonomic groups in Fig. 4 (Therapsida, Temnospondyli, Archosauromorpha and Pareiasauridae).

The $\delta^{13}C_c$ values of bone and tooth apatite from Beaufort tetrapods ranges from −31.3‰ to −6.1‰. Those that have likely kept their pristine carbon isotope compositions (see discussion) were plotted against their age as bulk values in Fig. 5 and averages of the four taxonomic groups in Fig. 6.

In addition to SA50, SA09 (a rhinesuchid tooth sample from the *Tropidostoma* AZ) was discarded considering a drastically different $\delta^{13}C_c$ value from that of the bone of the same individual (SA10) and its anomalously low carbonate content for a tooth (0.88 wt.%).

Both $\delta^{18}O_p$ and $\delta^{13}C_c$ curves show comparable fluctuations during the studied time interval. The $\delta^{18}O_p$ values decrease slightly at the end of the *Pristerognathus* AZ and show a sharp increase of about 4‰ during the middle-late Wuchiapingian, followed by a ~5‰ decrease at the End Permian. The Permo-Triassic boundary is characterized by an abrupt positive shift in $\delta^{18}O_p$ values of about 8‰. Oxygen isotope compositions stay high and steady until the early Anisian before they decrease down to values similar to those recorded at the end of the Permian (Fig. 4). Similar variations in $\delta^{18}O_p$ values are observed between the $\delta^{18}O_p$ curve of continental vertebrates from the Karoo Basin and those of marine conodonts from the Permian (Chen et al., 2013) and the Triassic (Joachimski et al., 2012; Sun et al., 2012; Trotter et al., 2015).

The $\delta^{13}C_c$ values peak at −8‰ during the Capitanian, then show a continuous decrease of about 10‰ until the late Wuchiapingian, followed by a positive excursion at the end of the stage. The end-Permian is characterized by a slight decrease in $\delta^{13}C_c$ values that reach about −16‰ followed by an abrupt increase of about 4‰ at the Permo-Triassic boundary. Similar to the $\delta^{18}O_p$ curve, $\delta^{13}C_c$ values stay high until the early Anisian,

Please cite this article as: Rey, K., et al., Global climate perturbations during the Permo-Triassic mass extinctions recorded by continental tetrapods from South Africa, Gondwana Research (2015), http://dx.doi.org/10.1016/j.gr.2015.09.008

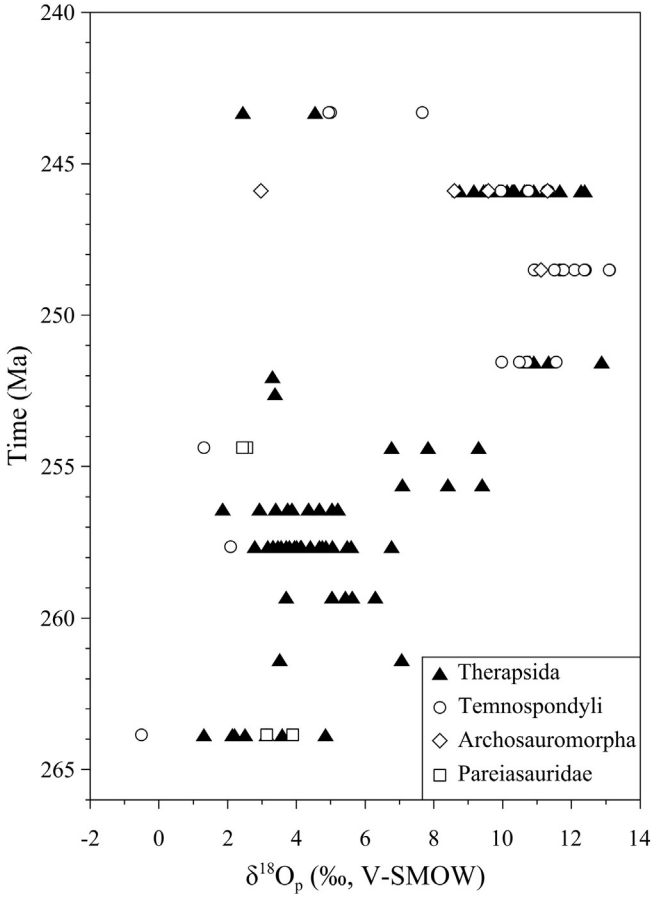

Fig. 3. Apatite $\delta^{18}O_p$ values of Karoo tetrapods plotted against the estimated age of their Formation/Assemblage Zone.

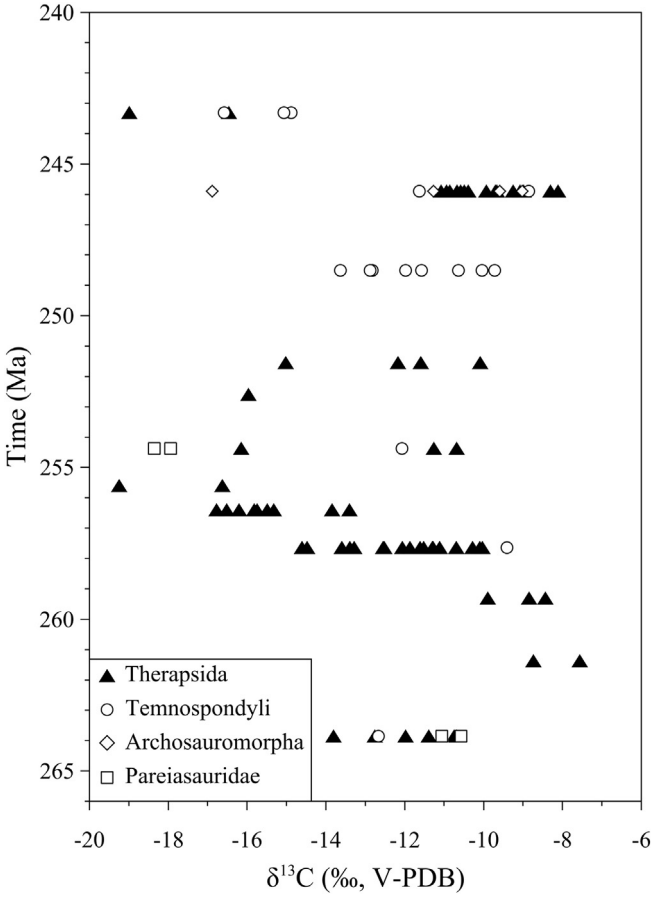

Fig. 5. Apatite $\delta^{13}C$ values of Karoo tetrapods plotted against the estimated age of their Formation/Assemblage Zone.

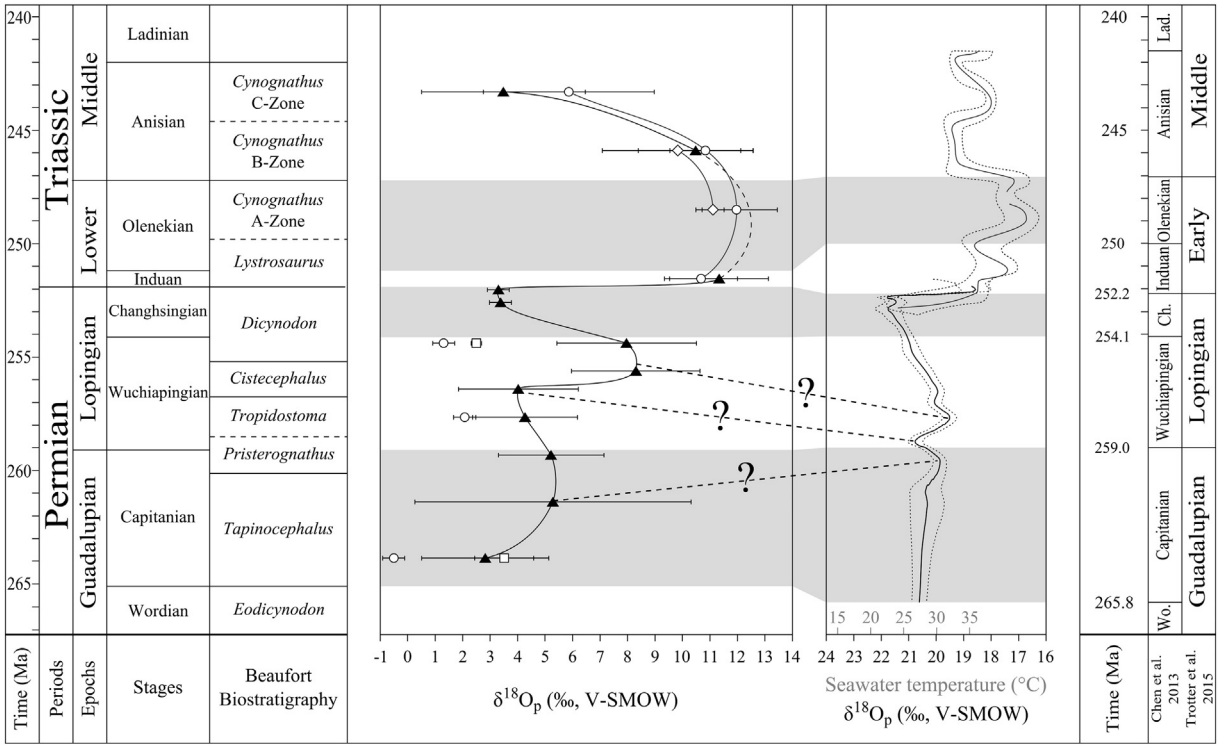

Fig. 4. Mean apatite $\delta^{18}O_p$ values of therapsids (black triangle) are compared to the marine conodont $\delta^{18}O_p$ curves from Chen et al. (2013) and Trotter et al. (2015). White circles, diamonds and squares represent mean $\delta^{18}O_p$ values of temnospondyls, archosauromorphs and pareiasaurids, respectively. Horizontal error-bars (tetrapods) and dotted lines (conodonts) represent calculated 95% confidence intervals. Bold dashed lines with "?" represent possible contemporaneous maxima and minima.

Please cite this article as: Rey, K., et al., Global climate perturbations during the Permo-Triassic mass extinctions recorded by continental tetrapods from South Africa, Gondwana Research (2015), http://dx.doi.org/10.1016/j.gr.2015.09.008

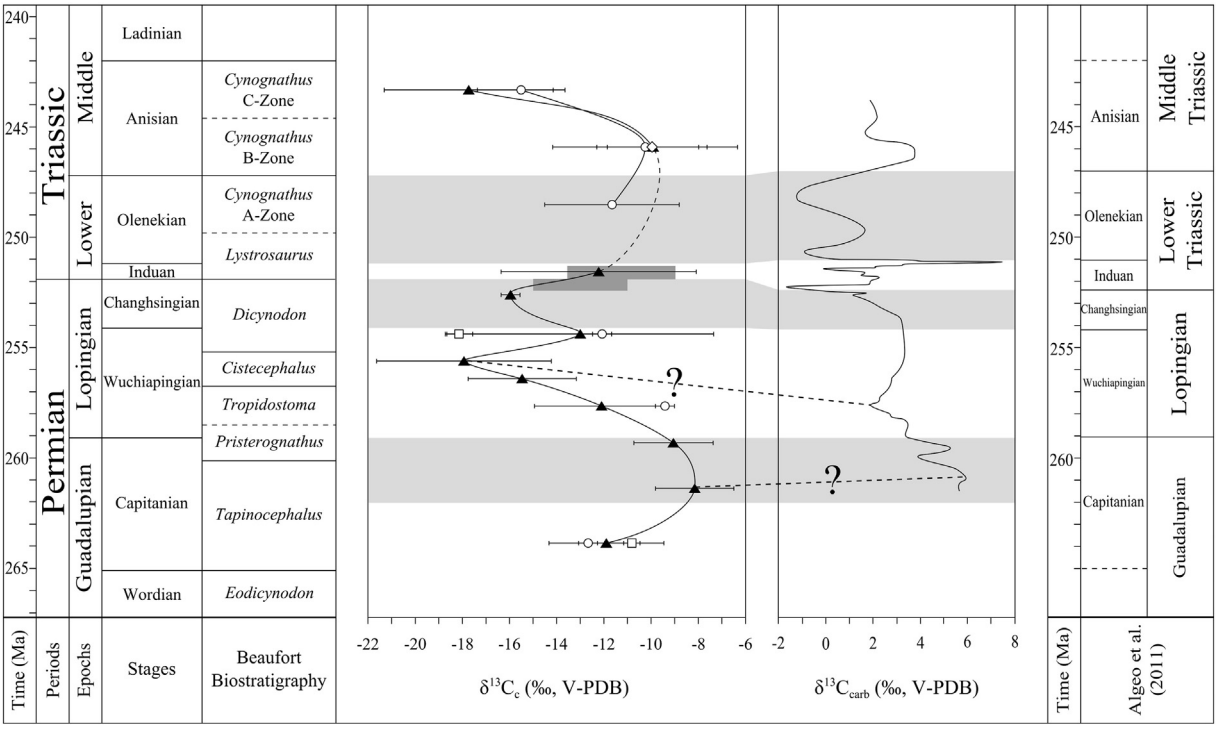

Fig. 6. Mean apatite $\delta^{13}C$ values of therapsids (black triangle) are compared to the marine carbonate $\delta^{13}C$ curve from Algeo et al. (2011). White circles, diamonds and squares represent mean $\delta^{13}C$ values of temnospondyls, archosauromorphs and pareiasaurids, respectively. Horizontal error-bars (tetrapods) represent calculated 95% confidence intervals. Bold dashed lines represent possible contemporaneous maxima and minima. Range in carbon isotope compositions of therapsid apatites from the Karoo Basin published by MacLeod et al. (2000) are represented as dark gray rectangles.

then decrease down to −18‰ (Fig. 6). This $\delta^{13}C_c$ curve shows similarities with the composite $\delta^{13}C$ curve of marine carbonates of Algeo et al. (2011) who compiled data from Payne et al. (2004), Isozaki et al. (2007b), Korte et al. (2005a,b) and Korte and Kozur (2010).

4. Discussion

4.1. Robustness of the stable isotope record

All samples that were used for this study were taken from either bones or tooth dentine. The apatite found within these materials is more porous than in enamel and the crystals are smaller and less densely intergrown (Brudefold and Soremark, 1967; Trautz, 1967). Thus, their original stable isotope compositions are more prone to modification through diagenetic processes. Alteration may take place through three main processes, which are 1) precipitation of secondary minerals within and at the surface of bioapatite crystals, 2) adsorption of ions on the surface of apatite crystals, and 3) dissolution and recrystallization with isotopic exchange.

Although no method is available to determine with certainty whether or not the stable isotope compositions of fossil vertebrate bioapatite has been modified by diagenetic processes, several protocols have been used to assess the fidelity of bioapatite carbonate $\delta^{18}O_c$ and $\delta^{13}C_c$ values. Broadly speaking, the carbonate content in the dental and osteological apatite of modern vertebrates typically ranges from about 2% to 13.4% (Brudefold and Soremark, 1967; Rink and Schwarcz, 1995; Vennemann et al., 2001), although it can be less than 1% in some bones (e.g., Tarnowski et al., 2002). Thus, fossil bone and dentine samples that have carbonate contents exceeding 13.4 wt.% likely contain additional inorganic carbonate precipitated from diagenetic fluids that was not removed during pre-treatment. Consequently, both oxygen and carbon isotope data obtained from these samples can be discarded (Fig. 7).

Pristine preservation of the oxygen isotope composition of apatite phosphate can also be tested using the method proposed by Iacumin et al. (1996). In modern vertebrates, the oxygen isotope compositions

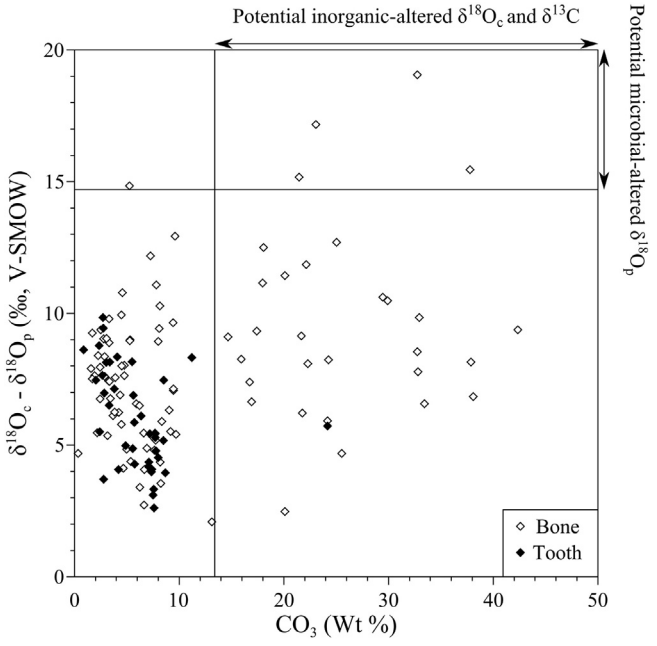

Fig. 7. $\delta^{18}O_c$–$\delta^{18}O_p$ differences between teeth and bones plotted against the structural carbonate content (wt.%) of apatite. Samples that have $\delta^{18}O_c$–$\delta^{18}O_p$ differences higher than 14.7‰ (Vennemann et al., 2001) are considered doubtful regarding a potential diagenetic alteration (see text). For carbonate contents (wt%) higher than 13.4, the $\delta^{18}O_c$ and $\delta^{13}C$ values are considered to have been altered by inorganic diagenetic processes (Zazzo et al., 2004a), whereas a too high difference between $\delta^{18}O_c$ and $\delta^{18}O_p$ is interpreted as a microbially-mediated alteration of the apatite phosphate (Zazzo et al., 2004a) or too high $\delta^{18}O_c$ values resulting from the addition of inorganic carbonate or isotopic exchange with an external source of inorganic carbon.

Please cite this article as: Rey, K., et al., Global climate perturbations during the Permo-Triassic mass extinctions recorded by continental tetrapods from South Africa, Gondwana Research (2015), http://dx.doi.org/10.1016/j.gr.2015.09.008

of apatite carbonate are normally between 7 and 9‰ higher than the $\delta^{18}O_p$ values of co-occurring apatite phosphate (e.g., Longinelli and Nuti, 1973; Bryant et al., 1996; Iacumin et al., 1996; Shahack-Gross et al., 1999; Zazzo et al., 2004b; Lécuyer et al., 2010; Chenery et al., 2012), although they can be as much as 14.7‰ greater (Vennemann et al., 2001). Zazzo et al. (2004a) have shown that microbially-mediated diagenetic alteration of apatite phosphate results in a higher discrepancy between $\delta^{18}O_c$ and $\delta^{18}O_p$ values. In this manner, fossil samples exhibiting $\delta^{18}O_c$–$\delta^{18}O_p$ discrepancies greater than 14.7‰ are almost certainly altered and can be discarded (Fig. 7). Inorganic alteration at low temperature has little effect on the $\delta^{18}O_p$ values of phosphates, even at geological time scales (Tudge, 1960; Lécuyer et al., 1999), so samples affected by inorganic diagenetic alteration of carbonates, (resulting either in a high overall carbonate content or in a low $\delta^{18}O_c$–$\delta^{18}O_p$ discrepancies), may still preserve the original oxygen isotope composition of their phosphates (Fig. 7). Using these two assessments, five $\delta^{18}O_p$ values out of 134 samples have been discarded, as well as 33 carbonate $\delta^{13}C_c$ and $\delta^{18}O_c$ values out of 136.

For 20 fossil specimens, the oxygen and carbon isotope compositions of their teeth have been compared to those of their corresponding bones (Figs. 8 and 9). Considering that all sampled tetrapod lineages continuously replaced their teeth (polyphyodont), it is expected that the mineralization timing of their bones is almost synchronous to that of their functional teeth. Both their bones and teeth should therefore have similar oxygen and carbon isotope compositions. Accordingly, samples that have likely preserved the oxygen and carbon isotope compositions of both phosphate and carbonate according to the first two tests should have the same bone and teeth stable isotope compositions (Figs. 8 and 9). As expected, samples for which carbonate contents indicate addition of diagenetic carbonate display similar bone and tooth $\delta^{18}O_p$ values (Fig. 8) whereas their tooth and bone carbon isotope compositions differ (Fig. 9).

From these considerations, at least partial preservation of the original stable oxygen isotope compositions of phosphate and carbon isotope composition of carbonates in selected samples can be accepted.

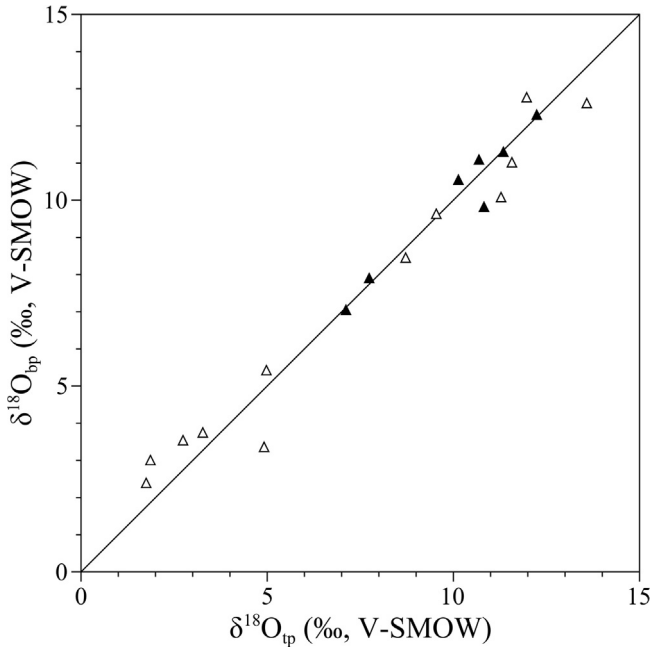

Fig. 8. Bone $\delta^{18}O_{bp}$ values are plotted against tooth $\delta^{18}O_{tp}$ values belonging to the same individual. White triangles correspond to samples having $\delta^{18}O_p$ values considered as pristine (see text and Fig. 7). Black triangles correspond to samples with a too high proportion of structural apatite carbonate but with a $\delta^{18}O_c$–$\delta^{18}O_p$ difference lower than 14.7‰. Interestingly, samples having too high structural apatite carbonate contents (black triangles) still have $\delta^{18}O_p$ values that fall within the expected preserved values, and are considered to have preserved their original isotope compositions.

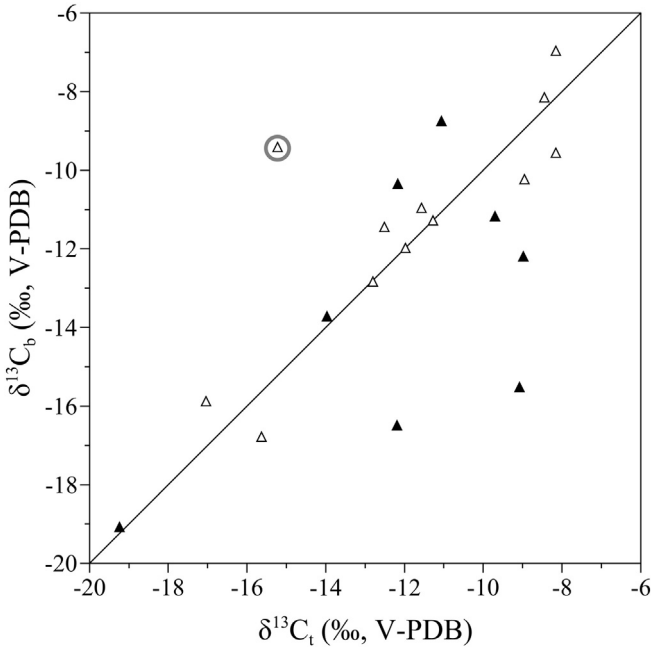

Fig. 9. Bone $\delta^{13}C_{bc}$ values are plotted against tooth $\delta^{13}C_{tc}$ values belonging to the same individual. White triangles correspond to samples having $\delta^{18}O_p$ values considered as pristine (see text and Fig. 7). Black triangles correspond to samples with a too high proportion of structural apatite carbonate but with a $\delta^{18}O_c$–$\delta^{18}O_p$ difference lower than 14.7‰. The circled white triangle represents an outlier for which tooth sample SA09 was removed from the database for subsequent interpretations (see text). Samples having too high structural apatite carbonate contents (black triangles) have $\delta^{13}C$ values that do not fall within the expected preserved values as a result of diagenetic alteration.

4.2. Ecological influences on the stable isotope composition of tetrapods

Even after postdepositional alteration is discounted, the ecophysiology of the different taxonomic groups (and individual species) may have influenced the isotopic signature of their hard tissues. Among the most common tetrapods in the Beaufort Group, and thus the most sampled in this study, are therapsids, which are represented by five primary taxonomic divisions: Dinocephalia, Therocephalia, Gorgonopsia, Anomodontia (including Dicynodontia) and Cynodontia. Genera of these groups display a variety of body masses, diets and probably a range of thermo-metabolic strategies. They all share a terrestrial habitat (Kammerer, 2011; Kemp, 2012; Smith et al., 2012) with some possibly being more specialized species such as riparian anteosaurs (Boonstra, 1955, 1962), or fossorial dicynodonts and cynodonts (eg. *Diictodon*, *Thrinaxodon*; Smith et al., 2012; Fernandez et al., 2013). These differences might result in variations in both oxygen and carbon isotope ratios in their biogenic apatite. For example, the uppermost two subzones of the *Cynognathus* AZ contain both cynodonts and dicynodonts. The former are inferred to possess higher metabolic rates than dicynodonts based on morphological features such as their more erect gait, possession of nasal turbinal complexes, and bone histology (Bennett and Ruben, 1986; Ruben, 1995). Cynodonts in these subzones have $\delta^{18}O_p$ values about 2‰ higher than coexisting dicynodonts, a difference that could result from a more important production of ^{18}O-enriched metabolic water in cynodonts.

Parareptiles are represented by two to three pareiasaurid genera, considering that the indeterminate pareiasaurids from the Lower *Tapinocephalus* AZ could belong to any of the basal genera *Bradysaurus*, *Embrithosaurus* or *Nochelosaurus* (Lee, 1997). Interpretations of the life habits and habitats of pareiasaurs still lack consensus, some authors considering them as fully aquatic (Ivakhnenko, 2001), others as semi-aquatic (Khlyupin, 2007; Kriloff et al., 2008) or fully terrestrial (Voigt et al., 2010; Benton et al., 2012; Canoville et al., 2014). An aquatic lifestyle would imply increased water turnover as well as much less

Please cite this article as: Rey, K., et al., Global climate perturbations during the Permo-Triassic mass extinctions recorded by continental tetrapods from South Africa, Gondwana Research (2015), http://dx.doi.org/10.1016/j.gr.2015.09.008

water loss through trans-cutaneous evaporation, leading to significantly lower $\delta^{18}O_p$ values in aquatic animals compared to fully terrestrial ones (e.g., Bocherens, 1996; Amiot et al., 2010). Indeterminate pareiasaurid specimens from the Lower *Tapinocephalus* AZ have $\delta^{18}O_p$ values within the range of coexisting terrestrial therapsids, suggesting a terrestrial lifestyle. On the other hand, *Pareiasaurus* specimens from the Lower *Dicynodon* AZ have $\delta^{18}O_p$ values 6‰ lower than coexisting therapsids, and close to that of coexisting amphibians, suggesting a semi-aquatic to aquatic lifestyle (Fig. 3).

Sampled temnospondyl amphibians represent at least seven genera, all from the clade Stereospondyli. Whereas most of them are regarded as fully aquatic (Schoch, 2009), some have been identified as more terrestrial (Fernandez et al., 2013; Canoville and Chinsamy, 2015). It is therefore predicted that their oxygen isotope composition would be lower than those of coexisting terrestrial reptiles, which is the case in all analyzed Permian amphibians (Fig. 3). Surprisingly, Triassic temnospondyls $\delta^{18}O_p$ values are similar to, or more positive than, those of coexisting terrestrial reptiles. Larger body size in some Triassic temnospondyls (Schoch, 2009) with "high walking" locomotion and the trend toward increased global aridity resulting in ^{18}O-enriched living waters (e.g., Benton and Newell, 2014; Viglietti et al., 2013) may account for these non-intuitive differences in $\delta^{18}O_p$ values. A dedicated investigation of the ecology of these amphibians should allow a better understanding of the unexpected oxygen isotope composition of their skeletal phosphate.

Archosauromorphs are represented by the Erythrosuchidae with *Erythrosuchus* restricted to the *Cynognathus* subzone B and *Garjainia* to subzone A. Erythrosuchids were the largest terrestrial predators of their time (Gower et al., 2014), and according to paleohistological studies, this taxon may have achieved some kind of thermoregulation through metabolic activity (de Ricqlès et al., 2003; Gower et al., 2014). Assuming therapsids probably display a range of thermo-metabolic strategies, it would be expected that archosaurs and therapsids exhibit a similar range of $\delta^{18}O_p$ values.

Considering all those possible ecological biases of the analyzed tetrapods, the variations in both $\delta^{18}O_p$ and $\delta^{13}C_c$ values in terms of environmental evolution have been interpreted using values from therapsids only. Indeed, therapsid samples were available from all assemblage zones, except the *Cynognathus* Subzone A, and they are all assumed to belong to terrestrial species.

4.3. Mean annual temperature fluctuations during the Middle Permian–Middle Triassic interval

The oxygen isotope composition of apatite phosphate from tetrapods of the Beaufort Group ranges from −0.5‰ to +13.6‰. So far, all known oxygen isotope fractionation equations between vertebrate phosphate and water suggest that these low $\delta^{18}O_p$ values indicate that vertebrates ingested local waters with very negative oxygen isotope compositions (Amiot et al., 2007). It has been proposed that an average oxygen isotope composition of local surface waters can be roughly estimated by subtracting 21.9‰ from the average $\delta^{18}O_p$ value of vertebrate apatite in a given community (Amiot et al., 2004). The average $\delta^{18}O_p$ values of Karoo vertebrates range from 2.6 ± 3.0‰ in the Lower *Tapinocephalus* AZ to 11.9 ± 1.5‰ in subzone A of the *Cynognathus* AZ, so this method would suggest $\delta^{18}O$ values for local surface waters ranging from −19.3 ± 3.0‰ to −10.0 ± 1.5‰. Today the lowest mean meteoric water $\delta^{18}O$ values occur in mid- to high-latitude (50° to 75° lat.) climate zones ranging from Warm Summer Continental (or hemiboreal; existing in Eastern Europe and Eastern part of the USA–Canada frontier) to Polar (such as Northwest Territories of Canada) according to Köppen's classification (Peel et al., 2007). A hemiboreal climate is characterized by warm summers that can reach about 20 °C and very cold winters with sub-freezing to freezing temperatures, partly due to a strong continental effect, whereas Polar climate are characterized by a lack of warm summer (temperatures below 10 °C) and negative annual mean air temperatures. Moreover, the highest mean meteoric water $\delta^{18}O$ value of −10.0 ± 1.5‰ occurs today between latitudes 45° and 60° within a hemiboreal climatic belt.

Estimated meteoric water $\delta^{18}O$ values as low as −19.3‰ for the middle Permian are relatively low, and today would occur only in climate zones with very low mean air temperatures. Such climatic conditions during the middle Permian may be unlikely given the presence of a diverse reptile fauna and sedimentological evidence for warm semi-arid environments (Smith and Botha-Brink, 2014) although it is possible that they possessed thermoregulatory strategies enabling them to cope with cold climatic conditions (high thermo-metabolism, hibernation). Another possibility is that local surface waters ingested by vertebrates originate from high altitude rainfall which is commonly ^{18}O-depleted relative to those from low latitudes. A mountainous origin for these waters is likely as sediments constituting the Beaufort Group come from either the Cape Fold Belt or the hypothetic "Eastern Highland" (Smith, 1995). Therefore, local water $\delta^{18}O$ values may not directly reflect local temperatures, but those of nearby high altitude areas. However, temporal variation in local water $\delta^{18}O$ values should reflect local air temperature variations, if we assume a homogeneous source of meteoric water supply throughout the studied time interval. Modern relationships show that mean air temperatures (MAT) are related to the average $\delta^{18}O_{mw}$ values of meteoric waters with a $\delta^{18}O_{mw}$/MAT slope of about 0.48 (Lécuyer, 2014).

In order to identify whether South African tetrapods have recorded global climatic conditions in their oxygen isotope compositions, their $\delta^{18}O_p$ curve is compared to that of available marine records. Several studies have investigated temperature variation across the Permo-Triassic interval in the marine realm using stable oxygen isotopes from low-Mg calcite of brachiopods (Korte et al., 2005a,b; 2008) or from conodont phosphate (Joachimski et al., 2012; Sun et al., 2012; Chen et al., 2013; Trotter et al., 2015). Because conodont $\delta^{18}O_p$ curves are limited to samples from areas within a restricted latitudinal range, thus reducing the variability induced by the latitudinal thermal gradient, the comparison will focus on the work of Chen et al. (2013) who proposed a curve for the Permian of South China, as well as on the curve proposed by Trotter et al. (2015) for the Triassic of Turkey and the Southern Alps (Fig. 10). Because of possible variations in sedimentation and compaction rates in both continental and marine sediments, we have restricted the comparison between the two curves at the stage resolution and, as mentioned above, only the $\delta^{18}O_p$ variation in therapsids is considered. At the first order, the two records vary similarly, suggesting that variations in oxygen isotope composition of Karoo therapsids reflect global climatic trends (Fig. 4).

The Capitanian–Wuchiapingian transition is characterized by a slight decrease in continental $\delta^{18}O_p$ values of 1.3 ± 4.1‰ (2σ) that could correspond to a global temperature drop of 3 ± 9 °C if we consider the present-day $\delta^{18}O_{mw}$/MAT slope of 0.48. However, it is most likely that this present-day relationship does not apply to the Permian. For example, lower slopes down to 0.36 ± 0.11 and 0.39 ± 0.24 have been established for the Eocene of North America (Secord et al., 2010). If such lower slopes applied to the Permian, especially during periods characterized by the absence of polar ice caps, temperature differences would have been about 3.5 ± 11 °C. This cooling event is also recorded in conodont $\delta^{18}O_p$ values with a calculated temperature decrease of 6 to 8 °C (Chen et al., 2013) that compares to estimates inferred from tetrapod $\delta^{18}O_p$ values. Such a cooling event has been associated with the Capitanian mass extinction, probably triggered by the Emeishan volcanism (Ali et al., 2002; Zhou et al., 2002; Wignall et al., 2009). Isozaki et al. (2007a,b) also identified a period of reduced temperatures in the Capitanian that they called the "Kamura effect" which coincided with a major sea-level fall (e.g., Hallam and Wignall, 1999; Tong et al., 1999; Kofukuda et al., 2014).

During the Wuchiapingian, continental tetrapod $\delta^{18}O_p$ values increased by 4.3 ± 4.5‰ corresponding to a temperature increase of 9 ± 9 °C that is also recognized in the marine record as a global warming

Please cite this article as: Rey, K., et al., Global climate perturbations during the Permo-Triassic mass extinctions recorded by continental tetrapods from South Africa, Gondwana Research (2015), http://dx.doi.org/10.1016/j.gr.2015.09.008

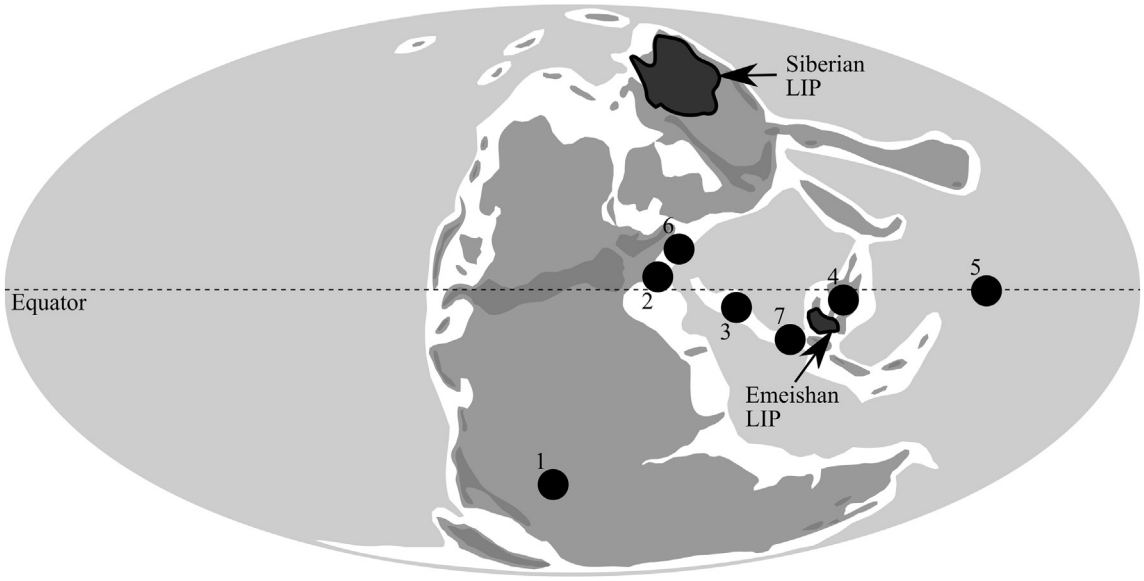

Fig. 10. Late Permian paleogeographic map showing the location of sampled tetrapods from the Karoo Basin (1), as well as samples of marine conodonts from the Southern Alps, the Sicani Basin and the Lagonegro Basin (2; Trotter et al., 2015), Turkey (3; Trotter et al., 2015) and South China (4; Joachimski et al., 2012; Sun et al., 2012; Chen et al., 2013). The location of marine carbonate samples from South China (4; Payne et al., 2004), Japan (5; Isozaki et al., 2007a,b), Hungary, Germany, Poland and France (6; Korte et al., 2005b) and Iran (7; Korte et al., 2005a; Korte and Kozur, 2010) are also reported. LIP: Large Igneous Province. Map modified from Grasby et al. (2011).

event (Isozaki et al., 2007a,b; Chen et al., 2011; Kofukuda et al., 2014). Warm conditions prevailing during part of the Lopingian is followed both in continents and oceans by a cooling of 10 ± 6 °C in continental South Africa and of about 9 °C in oceans (Chen et al., 2013) that lasted until the end Permian. According to Chen et al. (2013), this temperature drop seems unrealistic and would be the consequence of a bathymetric change of analyzed conodonts into cooler deeper waters. The present dataset, however, suggests the occurrence of an important cooling that affected both continents and oceans.

The Permo-Triassic boundary is marked by an abrupt and intense warming of 17 ± 5 °C recorded in Karoo tetrapod $\delta^{18}O_p$ values (Fig. 4). A similar warming of about 20 °C is estimated from low latitude conodonts (Joachimski et al., 2012; Sun et al., 2012; Trotter et al., 2015), although Trotter et al. (2015) considered that additional controls on the $\delta^{18}O_p$ values may have contributed to the isotope shift, thus overestimating the temperature increase. In the Karoo Basin, increased aridity during the Early Triassic may have contributed to the observed positive shift of about 8‰ in apatite $\delta^{18}O_p$ values. Indeed, evaporation of surface waters drunk by vertebrates, as well as body water loss through trans-cutaneous evaporation lead to ^{18}O-enriched oxygen isotope compositions of apatite phosphate. This would result in overestimation of local temperatures. However, the contribution of local aridity to the oxygen isotope composition of apatite phosphate is difficult to estimate. The fact that the estimated temperature increase is similar for both continental vertebrates and marine conodonts would favor the possibility that most of the isotopic signal derives from temperature. The likely explanation of this abrupt temperature rise is the volcanic release into the atmosphere of greenhouse gasses such as CO_2 or CH_4 in relation to the building of the Siberian Traps (Retallack and Jahren, 2008; Grasby et al., 2011; Sobolev et al., 2011; Sanei et al., 2012). It has also been proposed that methane release from permafrost and marine clathrates (De Wit et al., 2002; Heydari and Hassanzadeh, 2003; Ryskin, 2003; Retallack et al., 2003), or gas released by coal-beds cross-cut by igneous intrusions (McElwain et al., 2005; Retallack et al., 2006; Retallack and Jahren, 2008) could have contributed to this major climate perturbation. According to conodont $\delta^{18}O_p$ values from low latitudes (Fig. 10), seawater temperatures remained high until the end of the Early Triassic (Trotter et al., 2015). Tetrapods from the Karoo Basin also record high air temperatures followed by a 16 ± 10 °C drop during the Anisian, also indicated by conodont $\delta^{18}O_p$ values with a >6 °C decrease in marine temperatures (Fig. 4; Trotter et al., 2015).

4.4. Local environmental conditions inferred from apatite $\delta^{13}C_c$ values

The temporal evolution of the carbon isotope composition of tetrapod apatite is compared to a composite curve of low latitude marine carbonate $\delta^{13}C$ values compiled by Algeo et al. (2011) using data from Payne et al. (2004), Isozaki et al. (2007b), Korte et al. (2005a,b) and Korte and Kozur (2010; Figs. 06 and 10). Marine carbonate $\delta^{13}C$ values reflect those of atmospheric CO_2, a 1‰ variation in the atmosphere corresponding to a 1‰ variation in the carbonates with a seawater carbonate-atmosphere ^{13}C-enrichment factor of 9.3‰ (Cui et al., 2013).

The carbon isotope composition of continental vertebrate apatite ultimately reflects that of local vegetation with a ^{13}C-enrichment depending on trophic level and digestive physiology (Koch et al., 1994; Cerling and Harris, 1999; Passey et al., 2005). It is assumed that Permian and Triassic plants were exclusively using the C_3 photosynthetic pathway, thus their $\delta^{13}C$ values mostly reflect the carbon isotope composition of atmospheric CO_2 (Farquhar et al., 1982), although this can be influenced by local humidity as plant $\delta^{13}C$ values for C_3 plants increase under water stress (Farquhar et al., 1982). Comparing variations in $\delta^{13}C$ values of continental vertebrate apatite with those of marine carbonates can therefore be used to test for aridity. The Capitanian–Wuchiapingian interval is characterized by a drop of 9.8 ± 5.4‰ in Karoo tetrapod $\delta^{13}C_c$ values whereas marine carbonates record only a 4‰ drop (Fig. 6). Interestingly, a similar 9–10‰ decrease in apatite $\delta^{13}C_c$ values has also been measured in South African *Diictodon feliceps* tusks (Thackeray et al., 1990). After subtracting the 4‰ decrease in atmospheric $\delta^{13}C$ values to the ~10‰ drop in Karoo tetrapod $\delta^{13}C_c$ values, the remaining ~6‰ suggests that increasingly humid conditions may have occurred throughout the Wuchiapingian. Those conditions have also been observed by Retallack (2005) who interpreted an increase in the mean annual precipitation of the Karoo Basin during the Wuchiapingian using paleosols. From the end of the Wuchiapingian to the end of the Permian, the very few samples available so far preclude any robust interpretation of tetrapod $\delta^{13}C_c$ values. In oceanic carbonate records, the Changhsingian is characterized by another ~4‰ decrease in $\delta^{13}C$ values followed by fluctuating conditions during the Early and Middle Triassic (Fig. 6). In the Karoo Basin, the Permian to Triassic

Please cite this article as: Rey, K., et al., Global climate perturbations during the Permo-Triassic mass extinctions recorded by continental tetrapods from South Africa, Gondwana Research (2015), http://dx.doi.org/10.1016/j.gr.2015.09.008

transition shows a 6.0 ± 2.4‰ positive shift in tetrapod $\delta^{13}C_c$ values, reflecting more arid conditions lasting until the end of the Early Triassic. We emphasize that our dataset for the base of the Triassic is based on a single locality and cannot capture the environmental variations recorded in marine data. However, the value range (−16.4‰ to −8.1‰) is similar to the range measured at higher temporal resolution on therapsids by MacLeod et al. (2000) for the Lower Induan (−15‰ to −9‰). MacLeod et al. (2000) observed a negative peak similar to the marine record. The earliest Triassic is characterized by a climate drier than during the Late Permian with a semi-arid and highly seasonal climate with maximal mean temperatures up to 15–20 °C (Viglietti et al., 2013). Both continental and marine curves suggest similar climate modes during the entire Early Triassic, with possible fluctuations identified in the marine record.

5. Concluding remarks

In order to investigate environmental conditions that prevailed during the deposition of the Permo-Triassic Beaufort Group in South Africa, stable oxygen and carbon isotope compositions of vertebrate apatite recovered from 13 stratigraphic levels were analyzed. The following results are highlighted:

- Primary preservation of the original stable oxygen and carbon isotope compositions of vertebrate bone and tooth apatite has been positively assessed for the majority of analyzed samples.
- The relatively close trends in the curves resulting from our work on tetrapod bones from the continental realm and those from previously published work from fossils in the marine realm over the same period suggest that Karoo vertebrates have recorded the fluctuations of global temperatures.
- Interpolated mean annual air temperatures of the main Karoo Basin are characterized by an abrupt increase of about + 8 °C during the end of the Wuchiapingian that took place within a weak cooling trend from the Capitanian to the Permo-Triassic boundary. The end Permian is characterized by an intense and rapid warming period of + 16 °C that extended until the Olenekian. Atmospheric temperatures finally decreased during the Anisian and returned to pre-PTB values.
- Reconstructed temperature fluctuations and their magnitudes may be related to the Emeishan (South China) and Siberian paroxysmal volcanic events that took place at the end Capitanian and end Wuchiapingian, respectively.
- Carbon isotope compositions of terrestrial vertebrate apatite partly reflect the important fluctuations of atmospheric $\delta^{13}C$ values, the differences with the curves from the marine realm probably being due to the development of local humidity. According to these curves, local environments became more humid during the Capitanian–Wuchiapingian interval, and became more arid during the Lower Triassic before decreasing toward pre-Triassic values during the Late Anisian.

Acknowledgments

The authors would like to thank the two anonymous reviewers for their constructive comments that greatly helped to improve the first draft of this manuscript. We also would like to thank the Iziko South African Museum and the Evolutionary Studies Institute for granting access to the fossils and the South African Heritage Resources Agency (SAHRA) for their authorizations to sample and export fossils for stable isotope analysis (PermitID: 1858). We also would like to thank Dr. Guillaume Suan for the constructive discussion that helped to improve the manuscript. This work was supported by a French project INSU of the Centre National de la Recherche Scientifique, Palaeontological Scientific Trust (PAST) and its Scatterlings of Africa programs, National Research Foundation (NRF) and DST/NRF Centre of Excellence in Palaeosciences.

Appendix A. Supplementary data

Supplementary data to this article can be found online at http://dx.doi.org/10.1016/j.gr.2015.09.008.

References

Abdala, F., Ribeiro, A.M., 2010. Distribution and diversity patterns of Triassic cynodonts (Therapsida, Cynodontia) in Gondwana. Palaeogeography, Palaeoclimatology, Palaeoecology 286, 202–217. http://dx.doi.org/10.1016/j.palaeo.2010.01.011.

Algeo, T.J., Chen, Z.Q., Fraiser, M.L., Twitchett, R.J., 2011. Terrestrial–marine teleconnections in the collapse and rebuilding of Early Triassic marine ecosystems. Palaeogeography, Palaeoclimatology, Palaeoecology 308, 1–11. http://dx.doi.org/10.1016/j.palaeo.2011.01.011.

Ali, J.R., Thompson, G.M., Song, X., Wang, Y., 2002. Emeishan Basalts (SW China) and the "end-Guadalupian" crisis: magnetobiostratigraphic constraints. Journal of the Geological Society 159, 21–29. http://dx.doi.org/10.1144/0016-764901086.

Alroy, J., 2008. Dynamics of origination and extinction in the marine fossil record. Proceedings of the National Academy of Sciences 105, 11536–11542. http://dx.doi.org/10.1073/pnas.0802597105.

Alroy, J., 2010. The shifting balance of diversity among major marine animal groups. Science 329, 1191–1194. http://dx.doi.org/10.1126/science.1189910.

Amiot, R., Buffetaut, E., Lecuyer, C., Wang, X., Boudad, L., Ding, Z., Fourel, F., Hutt, S., Martineau, F., Medeiros, M.A., Mo, J., Simon, L., Suteethorn, V., Sweetman, S., Tong, H., Zhang, F., Zhou, Z., 2010. Oxygen isotope evidence for semi-aquatic habits among spinosaurid theropods. Geology 38, 139–142. http://dx.doi.org/10.1130/G30402.1.

Amiot, R., Lécuyer, C., Buffetaut, E., Fluteau, F., Legendre, S., Martineau, F., 2004. Latitudinal temperature gradient during the Cretaceous Upper Campanian–Middle Maastrichtian: $\delta^{18}O$ record of continental vertebrates. Earth and Planetary Science Letters 226, 255–272. http://dx.doi.org/10.1016/j.epsl.2004.07.015.

Amiot, R., Lécuyer, C., Escarguel, G., Billon-Bruyat, J.-P., Buffetaut, E., Langlois, C., Martin, S., Martineau, F., Mazin, J.-M., 2007. Oxygen isotope fractionation between crocodilian phosphate and water. Palaeogeography, Palaeoclimatology, Palaeoecology 243, 412–420. http://dx.doi.org/10.1016/j.palaeo.2006.08.013.

Bambach, R.K., Knoll, A.H., Sepkoski, J.J., 2002. Anatomical and ecological constraints on Phanerozoic animal diversity in the marine realm. Proceedings of the National Academy of Sciences 99, 6854–6859. http://dx.doi.org/10.1073/pnas.092150999.

Barnes, C., Sweeting, C., Jennings, S., Barry, J.T., Polunin, N.V.C., 2007. Effect of temperature and ration size on carbon and nitrogen stable isotope trophic fractionation. Functional Ecology 21, 356–362. http://dx.doi.org/10.1111/j.1365-2435.2006.01224.x.

Bennett, A.F., Ruben, J.A., 1986. The Metabolic and Thermoregulatory Status of Therapsids. The Ecology and Biology of Mammal-like Reptiles. Smithsonian Institution Press, Washington, DC, pp. 207–218.

Benton, M.J., Newell, A.J., 2014. Impacts of global warming on Permo-Triassic terrestrial ecosystems. Gondwana Research 25, 1308–1337. http://dx.doi.org/10.1016/j.gr.2012.12.010.

Benton, M.J., Newell, A.J., Khlyupin, A.Y., Shumov, I.S., Price, G.D., Kurkin, A.A., 2012. Preservation of exceptional vertebrate assemblages in Middle Permian fluviolacustrine mudstones of Kotel'nich, Russia: stratigraphy, sedimentology, and taphonomy. Palaeogeography, Palaeoclimatology, Palaeoecology 319–320, 58–83. http://dx.doi.org/10.1016/j.palaeo.2012.01.005.

Bocherens, H., 1996. Isotopic biogeochemistry (^{13}C, ^{18}O) of mammalian enamel from African pleistocene hominid sites. Palaios 11, 306–318.

Bond, D.P.G., Hilton, J., Wignall, P.B., Ali, J.R., Stevens, L.G., Sun, Y., Lai, X., 2010. The Middle Permian (Capitanian) mass extinction on land and in the oceans. Earth-Science Reviews 102, 100–116. http://dx.doi.org/10.1016/j.earscirev.2010.07.004.

Bond, D.P.G., Wignall, P.B., Joachimski, M.M., Sun, Y., Savov, I., Grasby, S.E., Beauchamp, B., Blomeier, D.P.G., 2015. An abrupt extinction in the Middle Permian (Capitanian) of the Boreal Realm (Spitsbergen) and its link to anoxia and acidification. Geological Society of America Bulletin, B31216.1 http://dx.doi.org/10.1130/B31216.1.

Boonstra, L.D., 1962. The dentition of the titanosuchian dinocephalians. Annals of The South African Museum 46, 57–112.

Boonstra, L.D., 1955. The girdles and limbs of the South African Deinocephalia. Annals of The South African Museum 42, 185–326.

Botha-Brink, J., Huttenlocker, A.K., Modesto, S.P., 2014. Vertebrate paleontology of Nooitgedacht 68: A *Lystrosaurus maccaigi*-Rich Permo-Triassic boundary locality in South Africa. In: Kammerer, C.F., Angielczyk, K.D., Fröbisch, J. (Eds.), Early Evolutionary History of the Synapsida. Springer, Netherlands, pp. 289–304.

Botha, J., Smith, R.M.H., 2007. *Lystrosaurus* species composition across the Permo-Triassic boundary in the Karoo Basin of South Africa. Lethaia 40, 125–137. http://dx.doi.org/10.1111/j.1502-3931.2007.00011.x.

Brudefold, F., Soremark, R., 1967. Chemistry of the mineral phase of enamel—crystalline organization of dental mineral. Structural and Chemical Organization of Teeth. Miles AED, San Diego, pp. 247–277.

Bryant, J.D., Koch, P.L., Froelich, P.N., Showers, W.J., Genna, B.J., 1996. Oxygen isotope partitioning between phosphate and carbonate in mammalian apatite. Geochimica and Cosmochimica Acta 60, 5145–5148. http://dx.doi.org/10.1016/S0016-7037(96)00308-0.

Please cite this article as: Rey, K., et al., Global climate perturbations during the Permo-Triassic mass extinctions recorded by continental tetrapods from South Africa, Gondwana Research (2015), http://dx.doi.org/10.1016/j.gr.2015.09.008

Burgess, S.D., Bowring, S., Shen, S., 2014. High-precision timeline for Earth's most severe extinction. Proceedings of the National Academy of Sciences 111, 3316–3321. http://dx.doi.org/10.1073/pnas.1317692111.

Canoville, A., Chinsamy, A., 2015. Bone microstructure of the stereospondyl *Lydekkerina huxleyi* reveals adaptive strategies to the harsh post Permian-extinction environment. The Anatomical Record 298, 1237–1254. http://dx.doi.org/10.1002/ar.23160.

Canoville, A., Thomas, D.B., Chinsamy, A., 2014. Insights into the habitat of Middle Permian pareiasaurs (Pararreptilia) from preliminary isotopic analyses. Lethaia 47, 266–274.

Catuneanu, O., Hancox, P.J., Rubidge, B.S., 1998. Reciprocal flexural behaviour and contrasting stratigraphies: a new basin development model for the Karoo retroarc foreland system, South Africa. Basin Research 10, 417–439. http://dx.doi.org/10.1046/j.1365-2117.1998.00078.x.

Cerling, T.E., Harris, J.M., 1999. Carbon isotope fractionation between diet and bioapatite in ungulate mammals and implications for ecological and paleoecological studies. Oecologia 120, 347–363.

Chen, B., Joachimski, M.M., Shen, S., Lambert, L.L., Lai, X., Wang, X., Chen, J., Yuan, D., 2013. Permian ice volume and palaeoclimate history: oxygen isotope proxies revisited. Gondwana Research 24, 77–89. http://dx.doi.org/10.1016/j.gr.2012.07.007.

Chen, B., Joachimski, M.M., Sun, Y., Shen, S., Lai, X., 2011. Carbon and conodont apatite oxygen isotope records of Guadalupian–Lopingian boundary sections: climatic or sea-level signal? Palaeogeography, Palaeoclimatology, Palaeoecology 311, 145–153. http://dx.doi.org/10.1016/j.palaeo.2011.08.016.

Chenery, C.A., Pashley, V., Lamb, A.L., Sloane, H.J., Evans, J.A., 2012. The oxygen isotope relationship between the phosphate and structural carbonate fractions of human bioapatite. Rapid Communications in Mass Spectrometry 26, 309–319. http://dx.doi.org/10.1002/rcm.5331.

Clapham, M.E., Shen, S., Bottjer, D.J., 2009. The double mass extinction revisited: reassessing the severity, selectivity, and causes of the end-Guadalupian biotic crisis (Late Permian). Paleobiology 35, 32–50. http://dx.doi.org/10.1666/08033.1.

Cohen, K.M., Finney, S.M., Gibbard, P.L., Fan, J.-X., 2013. The ICS International Chronostratigraphic Chart. Episodes 36, 199–204.

Coney, L., Reimold, W.U., Hancox, P.J., Mader, D., Koeberl, C., McDonald, I., Struck, U., Vajda, V., Kamo, S.L., 2007. Geochemical and mineralogical investigation of the Permian–Triassic boundary in the continental realm of the southern Karoo Basin, South Africa. Palaeoworld 16, 67–104. http://dx.doi.org/10.1016/j.palwor.2007.05.003.

Crowson, R.A., Showers, W.J., Wright, E.K., Hoering, T.C., 1991. Preparation of phosphate samples for oxygen isotope analysis. Analytical Chemistry 63, 2397–2400. http://dx.doi.org/10.1021/ac00020a038.

Cui, Y., Kump, L.R., Ridgwell, A., 2013. Initial assessment of the carbon emission rate and climatic consequences during the end-Permian mass extinction. Palaeogeography, Palaeoclimatology, Palaeoecology 389, 128–136.

D'Angela, D., Longinelli, A., 1990. Oxygen isotopes in living mammal's bone phosphate: further results. Chemical Geology: Isotope Geoscience Section 86, 75–82. http://dx.doi.org/10.1016/0168-9622(90)90007-Y.

Dansgaard, W., 1964. Stable isotopes in precipitation. Tellus 16, 436–468. http://dx.doi.org/10.1111/j.2153-3490.1964.tb00181.x.

Day, M.O., 2013. Charting the fossils of the Great Karoo: a history of tetrapod biostratigraphy in the Lower Beaufort Group, South Africa. Palaeontologia Africana 48, 41–47.

Day, M.O., Ramezani, J., Bowring, S.A., Sadler, P.M., Erwin, D.H., Abdala, F., Rubidge, B.S., 2015. When and how did the terrestrial mid-Permian mass extinction occur? Evidence from the tetrapod record of the Karoo Basin, South Africa. Proceedings of the Royal Society of London B: Biological Sciences 282, 20150834.

De Kock, M.O., Kirschvink, J.L., 2004. Paleomagnetic constraints on the Permian–Triassic boundary in terrestrial strata of the Karoo Supergroup, South Africa: implications for causes of the end-Permian extinction event. Gondwana Research 7, 175–183. http://dx.doi.org/10.1016/S1342-937X(05)70316-6.

DeNiro, M., Epstein, S., 1978. Influence of diet on the distribution of carbon isotopes in animals. Geochimica and Cosmochimica Acta 42, 495–506. http://dx.doi.org/10.1016/0016-7037(78)90199-0.

de Ricqlès, A.J., Padian, K., Horner, J.R., 2003. On the bone histology of some Triassic pseudosuchian archosaurs and related taxa. Annales de Paleontologie 89, 67–101. http://dx.doi.org/10.1016/S0753-3969(03)00005-3.

Detian, Y., Liqin, Z., Zhen, Q., 2013. Carbon and sulfur isotopic fluctuations associated with the end-Guadalupian mass extinction in South China. Gondwana Research 24, 1276–1282. http://dx.doi.org/10.1016/j.gr.2013.02.008.

De Wit, M.J., Ghosh, J.G., De Villiers, S., Rakotosolofo, N., Alexander, J., Tripathi, A., Looy, C., 2002. Multiple organic carbon isotope reversals across the Permo-Triassic boundary of terrestrial Gondwana sequences: Clues to extinction patterns and delayed ecosystem recovery. The Journal of Geology 110. http://dx.doi.org/10.1086/338411.

Dustira, A.M., Wignall, P.B., Joachimski, M., Blomeier, D., Hartkopf-Fröder, C., Bond, D.P.G., 2013. Gradual onset of anoxia across the Permian–Triassic Boundary in Svalbard, Norway. Palaeogeography, Palaeoclimatology, Palaeoecology 374, 303–313. http://dx.doi.org/10.1016/j.palaeo.2013.02.004.

Ehleringer, J.R., Monson, R.K., 1993. Evolutionary and ecological aspects of photosynthetic pathway variation. Annual Review of Ecology and Systematics 411–439.

Erwin, D.H., 1993. The Great Paleozoic Crisis. Reprint edition. Columbia University Press, New York.

Farquhar, G.D., O'leary, M.H., Berry, J.A., 1982. On the relationship between carbon isotope discrimination and the intercellular carbon dioxide concentration in leaves. Functional Plant Biology 9, 121–137.

Fernandez, V., Abdala, F., Carlson, K.J., Cook, D.C., Rubidge, B.S., Yates, A., Tafforeau, P., 2013. Synchrotron reveals Early Triassic odd couple: injured amphibian and aestivating therapsid share burrow. PLoS ONE 8, e64978. http://dx.doi.org/10.1371/journal.pone.0064978.

Fildani, A., Weislogel, A., Drinkwater, N.J., McHargue, T., Tankard, A., Wooden, J., Hodgson, D., Flint, S., 2009. U–Pb zircon ages from the southwestern Karoo Basin, South Africa—implications for the Permian–Triassic boundary. Geology 37, 719–722. http://dx.doi.org/10.1130/G25685A.1.

Fourel, F., Martineau, F., Lécuyer, C., Kupka, H.-J., Lange, L., Ojeimi, C., Seed, M., 2011. $^{18}O/^{16}O$ ratio measurements of inorganic and organic materials by elemental analysis-pyrolysis-isotope ratio mass spectrometry continuous-flow techniques. Rapid Communications in Mass Spectrometry: RCM 25, 2691–2696. http://dx.doi.org/10.1002/rcm.5056.

Fricke, H.C., O'Neil, J.R., 1999. The correlation between $^{18}O/^{16}O$ ratios of meteoric water and surface temperature: its use in investigating terrestrial climate change over geologic time. Earth and Planetary Science Letters 170, 181–196. http://dx.doi.org/10.1016/S0012-821X(99)00105-3.

Gower, D.J., Hancox, P.J., Botha-Brink, J., Sennikov, A.G., Butler, R.J., 2014. A new species of Garjainia Ochev, 1958 (Diapsida: Archosauriformes: Erythrosuchidae) from the Early Triassic of South Africa. PLoS ONE 9, e111154. http://dx.doi.org/10.1371/journal.pone.0111154.

Grafenstein, U.V., Bocherens, H., Müller, J., Trimborn, P., Alefs, J., 1996. A 200 year mid-European air temperature record preserved in lake sediments: an extension of the $\delta^{18}O_p$–air temperature relation into the past. Geochimica and Cosmochimica Acta 60, 4025–4036. http://dx.doi.org/10.1016/S0016-7037(96)00230-X.

Grasby, S.E., Sanei, H., Beauchamp, B., 2011. Catastrophic dispersion of coal fly ash into oceans during the latest Permian extinction. Nature Geoscience 4, 104–107. http://dx.doi.org/10.1038/ngeo1069.

Groves, J.R., Wang, Y., 2013. Timing and size selectivity of the Guadalupian (Middle Permian) fusulinoidean extinction. Journal of Paleontology 87, 183–196. http://dx.doi.org/10.1666/12-076R.1.

Hallam, A., Wignall, P.B., 1999. Mass extinctions and sea-level changes. Earth-Science Reviews 48, 217–250. http://dx.doi.org/10.1016/S0012-8252(99)00055-0.

Hancox, P.J., Rubidge, B.S., 1996. The first specimen of the Mid-Triassic Dicynodont *Angonisaurus* from the Karoo of South Africa: implications for the dating and biostratigraphy of the *Cynognathus* Assemblage Zone, Upper Beaufort Group. South African Journal of Science 391–392.

Hancox, P.J., Shishkin, M.A., Rubidge, B.S., Kitching, J.W., 1995. A threefold subdivision of the *Cynognathus* Assemblage Zone (Beaufort Group, South Africa) and its palaeogeographical implications. South African Journal of Science 91, 143–144.

Heydari, E., Hassanzadeh, J., 2003. Deev Jahi Model of the Permian–Triassic boundary mass extinction: a case for gas hydrates as the main cause of biological crisis on Earth. Sedimentary Geology 163, 147–163. http://dx.doi.org/10.1016/j.sedgeo.2003.08.002.

Huang, C., Tong, J., Hinnov, L., Chen, Z.Q., 2011. Did the great dying of life take 700 k.y.? Evidence from global astronomical correlation of the Permian–Triassic boundary interval. Geology 39, 779–782. http://dx.doi.org/10.1130/G32126.1.

Huang, C., Tong, J., Hinnov, L., Chen, Z.Q., 2012. Did the great dying of life take 700 k.y.? Evidence from global astronomical correlation of the Permian–Triassic boundary interval: REPLY. Geology 40. http://dx.doi.org/10.1130/G33200Y.1 (e268-e268).

Iacumin, P., Bocherens, H., Mariotti, A., Longinelli, A., 1996. Oxygen isotope analyses of co-existing carbonate and phosphate in biogenic apatite: a way to monitor diagenetic alteration of bone phosphate? Earth and Planetary Science Letters 142, 1–6. http://dx.doi.org/10.1016/0012-821X(96)00093-3.

Isozaki, Y., 1997. Permo-Triassic boundary superanoxia and stratified superocean: records from lost deep sea. Science 276, 235–238.

Isozaki, Y., Kawahata, H., Minoshima, K., 2007a. The Capitanian (Permian) Kamura cooling event: the beginning of the Paleozoic–Mesozoic transition. Palaeoworld 16, 16–30. http://dx.doi.org/10.1016/j.palwor.2007.05.011.

Isozaki, Y., Kawahata, H., Ota, A., 2007b. A unique carbon isotope record across the Guadalupian–Lopingian (Middle–Upper Permian) boundary in mid-oceanic paleo-atoll carbonates: the high-productivity "Kamura event" and its collapse in Panthalassa. Global and Planetary Change 55, 21–38. http://dx.doi.org/10.1016/j.gloplacha.2006.06.006.

Ivakhnenko, M.F., 2001. Tetrapods from the east european placket—Late Paleozoic natural territorial complex. Tr. Paleontol. Inst. Ross. Akad. Nauk 283 pp. 1–200.

Jin, Y.G., Zhang, J., Shang, Q.H., 1994. Two phases of the end-Permian mass extinction. In: Embry, A.F., Beauchamp, B., Glass, D.J. (Eds.), Pangea: Global Environments and Resources. Memoir, pp. 818–822.

Joachimski, M.M., Lai, X., Shen, S., Jiang, H., Luo, G., Chen, B., Chen, J., Sun, Y., 2012. Climate warming in the latest Permian and the Permian–Triassic mass extinction. Geology 40, 195–198. http://dx.doi.org/10.1130/G32707.1.

Kammerer, C.F., 2011. Systematics of the Anteosauria (Therapsida: Dinocephalia). Journal of Systematic Palaeontology 9, 261–304. http://dx.doi.org/10.1080/14772019.2010.492645.

Kemp, T.S., 2012. The origin and radiation of Therapsids. In: Chinsamy-Turan, A. (Ed.), Forerunners of Mammals: Radiation, Histology, Biology, pp. 3–28 (Bloomington).

Khlyupin, A.Y., 2007. Cemetery of the Permian reptiles. Paleomir 1, 50–57.

Koch, P.L., Fogel, M.L., Tuross, N., 1994. Tracing the diets of fossil animals using stable isotopes. Stable isotopes in ecology and environmental sciencepp. 63–92.

Koch, P.L., Tuross, N., Fogel, M.L., 1997. The effects of sample treatment and diagenesis on the isotopic integrity of carbonate in biogenic hydroxylapatite. Journal of Archaeological Science 24, 417–430.

Kofukuda, D., Isozaki, Y., Igo, H., 2014. A remarkable sea-level drop and relevant biotic responses across the Guadalupian–Lopingian (Permian) boundary in low-latitude mid-Panthalassa: irreversible changes recorded in accreted paleo-atoll limestones in Akasaka and Ishiyama, Japan. Journal of Asian Earth Sciences 82, 47–65. http://dx.doi.org/10.1016/j.jseaes.2013.12.010.

Kohn, M.J., Schoeninger, M., Valley, J., 1996. Herbivore tooth oxygen isotope compositions: effects of diet and physiology. Geochimica and Cosmochimica Acta 60, 3889–3896. http://dx.doi.org/10.1016/0016-7037(96)00248-7.

Please cite this article as: Rey, K., et al., Global climate perturbations during the Permo-Triassic mass extinctions recorded by continental tetrapods from South Africa, Gondwana Research (2015), http://dx.doi.org/10.1016/j.gr.2015.09.008

Korte, C., Jasper, T., Kozur, H.W., Veizer, J., 2005a. $\delta^{18}O$ and $\delta^{13}C$ of Permian brachiopods: a record of seawater evolution and continental glaciation. Palaeogeography, Palaeoclimatology, Palaeoecology 224, 333–351. http://dx.doi.org/10.1016/j.palaeo.2005.03.015.

Korte, C., Jones, P.J., Brand, U., Mertmann, D., Veizer, J., 2008. Oxygen isotope values from high-latitudes: clues for Permian sea-surface temperature gradients and Late Palaeozoic deglaciation. Palaeogeography, Palaeoclimatology, Palaeoecology 269, 1–16. http://dx.doi.org/10.1016/j.palaeo.2008.06.012.

Korte, C., Kozur, H.W., 2010. Carbon-isotope stratigraphy across the Permian–Triassic boundary: a review. Journal of Asian Earth Sciences 39, 215–235. http://dx.doi.org/10.1016/j.jseaes.2010.01.005.

Korte, C., Kozur, H.W., Veizer, J., 2005b. $\delta^{13}C$ and $\delta^{18}O$ values of Triassic brachiopods and carbonate rocks as proxies for coeval seawater and palaeotemperature. Palaeogeography, Palaeoclimatology, Palaeoecology 226, 287–306. http://dx.doi.org/10.1016/j.palaeo.2005.05.018.

Kriloff, A., Germain, D., Canoville, A., Vincent, P., Sache, M., Laurin, M., 2008. Evolution of bone microanatomy of the tetrapod tibia and its use in palaeobiological inference. Journal of Evolutionary Biology 21, 807–826. http://dx.doi.org/10.1111/j.1420-9101.2008.01512.x.

Lécuyer, C., 2014. Water on Earth. John Wiley & Sons.

Lécuyer, C., Balter, V., Martineau, F., Fourel, F., Bernard, A., Amiot, R., Gardien, V., Otero, O., Legendre, S., Panczer, G., Simon, L., Martini, R., 2010. Oxygen isotope fractionation between apatite-bound carbonate and water determined from controlled experiments with synthetic apatites precipitated at 10–37 °C. Geochimica et Cosmochimica Acta 74, 2072–2081. http://dx.doi.org/10.1016/j.gca.2009.12.024.

Lécuyer, C., Fourel, F., Martineau, F., Amiot, R., Bernard, A., Daux, V., Escarguel, G., Morrison, J., 2007. High-precision determination of $^{18}O/^{16}O$ ratios of silver phosphate by EA-pyrolysis-IRMS continuous flow technique. Journal of Mass Spectrometry 42, 36–41. http://dx.doi.org/10.1002/jms.1130.

Lécuyer, C., Grandjean, P., O'Neil, J.R., Cappetta, H., Martineau, F., 1993. Thermal excursions in the ocean at the Cretaceous–Tertiary boundary (northern Morocco): $\delta^{18}O$ record of phosphatic fish debris. Palaeogeography, Palaeoclimatology, Palaeoecology 105, 235–243.

Lécuyer, C., Grandjean, P., Sheppard, S.M.F., 1999. Oxygen isotope exchange between dissolved phosphate and water at temperatures ≤135 °C: inorganic versus biological fractionations. Geochimica and Cosmochimica Acta 63, 855–862. http://dx.doi.org/10.1016/S0016-7037(99)00096-4.

Lee, M.S.Y., 1997. A taxonomic revision of pareiasaurian reptiles: implications for Permian terrestrial palaeoecology. Modern Geology 21, 231–298. http://dx.doi.org/10.1111/j.1096-3642.1997.tb01279.x.

Longinelli, A., Nuti, S., 1973. Oxygen isotope measurements of phosphate from fish teeth and bones. Earth and Planetary Science Letters 20, 337–340. http://dx.doi.org/10.1016/0012-821X(73)90007-1.

MacLeod, K.G., Smith, R.M.H., Koch, P.L., Ward, P.D., 2000. Timing of mammal-like reptile extinctions across the Permian–Triassic boundary in South Africa. Geology 28, 227. http://dx.doi.org/10.1130/0091-7613(2000)28<227:TOMREA>2.0.CO;2.

Maxwell, W.D., 1992. Permian and Early Triassic extinction of nonmarine tetrapods. Paleontology 35, 571–583.

McElwain, J.C., Wade-Murphy, J., Hesselbo, S.P., 2005. Changes in carbon dioxide during an oceanic anoxic event linked to intrusion into Gondwana coals. Nature 435, 479–482. http://dx.doi.org/10.1038/nature03618.

McGhee Jr., G.R., Clapham, M.E., Sheehan, P.M., Bottjer, D.J., Droser, M.L., 2013. A new ecological-severity ranking of major Phanerozoic biodiversity crises. Palaeogeography, Palaeoclimatology, Palaeoecology 370, 260–270. http://dx.doi.org/10.1016/j.palaeo.2012.12.019.

McLoughlin, S., Lindström, S., Drinnan, A.N., 1997. Gondwanan floristic and sedimentological trends during the Permian–Triassic transition: new evidence from the Amery Group, northern Prince Charles Mountains, East Antarctica. Antarctic Science 9, 281–298. http://dx.doi.org/10.1017/S0954102097000370.

Mundil, R., Ludwig, K.R., Metcalfe, I., Renne, P.R., 2004. Age and timing of the Permian mass extinctions: U/Pb dating of closed-system zircons. Science 305, 1760–1763.

Neveling, J., Hancox, P.J., Rubidge, B.S., 2005. Biostratigraphy of the lower Burgersdorp Formation (Beaufort Group; Karoo Supergroup) of South Africa—implications for the stratigraphic ranges of early Triassic tetrapods.

Nielsen, J.K., Shen, Y., 2004. Evidence for sulfidic deep water during the Late Permian in the East Greenland Basin. Geology 32, 1037–1040. http://dx.doi.org/10.1130/G20987.1.

Ochev, V.G., Shishkin, M.A., 1989. On the principles of global correlation of the continental Triassic on the tetrapods. Acta Palaeontologica Polonica 34, 149–173.

Passey, B.H., Robinson, T., Ayliffe, L., Cerling, T., Sponheimer, M., Dearing, M.D., Roeder, B.L., Ehleringer, J.R., 2005. Carbon isotope fractionation between diet, breath CO_2, and bioapatite in different mammals. Journal of Archaeological Science 32, 1459–1470. http://dx.doi.org/10.1016/j.jas.2005.03.015.

Payne, J.L., Lehrmann, D.J., Wei, J., Orchard, M.J., Schrag, D.P., Knoll, A.H., 2004. Large perturbations of the carbon cycle during recovery from the end-Permian extinction. Science 305, 506–509. http://dx.doi.org/10.1126/science.1097023.

Peel, M.C., Finlayson, B.L., McMahon, T.A., 2007. Updated world map of the Köppen-Geiger climate classification. Hydrology and Earth System Sciences 11, 1633–1644. http://dx.doi.org/10.5194/hess-11-1633-2007.

Quade, J., Cerling, T.E., Barry, J.C., Morgan, M.E., Pilbeam, D.R., Chivas, A.R., Lee-Thorp, J.A., van der Merwe, N., 1992. A 16-Ma record of paleodiet using carbon and oxygen isotopes in fossil teeth from Pakistan. Chemical Geology: Isotope Geoscience Section 94, 183–192. http://dx.doi.org/10.1016/0168-9622(92)90011-X.

Raup, D.M., Sepkoski, J.J., 1982. Mass extinctions in the marine fossil record. Science 215, 1501–1503. http://dx.doi.org/10.1126/science.215.4539.1501.

Retallack, G.J., 2005. Permian greenhouse crises. The Nonmarine Permian. New Mexico Museum of Natural History and Science Bulletin 30, 256–269.

Retallack, G.J., Jahren, A.H., 2008. Methane release from igneous intrusion of coal during Late Permian extinction events. The Journal of Geology 116, 1–20. http://dx.doi.org/10.1086/524120.

Retallack, G.J., Metzger, C.A., Greaver, T., Jahren, A.H., Smith, R.M.H., Sheldon, N.D., 2006. Middle-Late Permian mass extinction on land. Geological Society of America Bulletin 118, 1398–1411. http://dx.doi.org/10.1130/B26011.1.

Retallack, G.J., Smith, R.M.H., Ward, P.D., 2003. Vertebrate extinction across Permian–Triassic boundary in Karoo Basin, South Africa. Geological Society of America Bulletin 115, 1133–1152. http://dx.doi.org/10.1130/B25215.1.

Rink, W.J., Schwarcz, H.P., 1995. Tests for diagenesis in tooth enamel: ESR dating signals and carbonate contents. Journal of Archaeological Science 22, 251–255. http://dx.doi.org/10.1006/jasc.1995.0026.

Ruben, J., 1995. The evolution of endothermy in mammals and birds: from physiology to fossils. Annual Review of Physiology 57, 69–95. http://dx.doi.org/10.1146/annurev.ph.57.030195.000441.

Rubidge, B.S., 1995. Biostratigraphy of the Beaufort Group (Karoo Supergroup), Biostratigraphic Series. Geological Survey, Pretoria.

Rubidge, B.S., 2005. 27th Du Toit memorial lecture re-uniting lost continents—fossil reptiles from the ancient Karoo and their wanderlust. South African Journal of Geology 108, 135–172. http://dx.doi.org/10.2113/108.1.135.

Rubidge, B.S., Erwin, D.H., Ramezani, J., Bowring, S.A., de Klerk, W.J., 2013. High-precision temporal calibration of Late Permian vertebrate biostratigraphy: U–Pb zircon constraints from the Karoo Supergroup, South Africa. Geology 41, 363–366. http://dx.doi.org/10.1130/G33622.1.

Rubidge, B.S., Hancox, P.J., Catuneanu, O., 2000. Sequence analysis of the Ecca–Beaufort contact in the southern Karoo of South Africa. South African Journal of Geology 103, 81–96. http://dx.doi.org/10.2113/103.1.81.

Ryskin, G., 2003. Methane-driven oceanic eruptions and mass extinctions. Geology 31, 741–744.

Sahney, S., Benton, M.J., 2008. Recovery from the most profound mass extinction of all time. Proceedings of the Royal Society of London B: Biological Sciences 275, 759–765. http://dx.doi.org/10.1098/rspb.2007.1370.

Saitoh, M., Isozaki, Y., Yao, J., Ji, Z., Ueno, Y., Yoshida, N., 2013. The appearance of an oxygen-depleted condition on the Capitanian disphotic slope/basin in South China: Middle–Upper Permian stratigraphy at Chaotian in northern Sichuan. Global and Planetary Change 105, 180–192. http://dx.doi.org/10.1016/j.gloplacha.2012.01.002.

Sanei, H., Grasby, S.E., Beauchamp, B., 2012. Latest Permian mercury anomalies. Geology 40, 63–66. http://dx.doi.org/10.1130/G32596.1.

Schoch, R.R., 2009. Evolution of life cycles in early amphibians. Annual Review of Earth and Planetary Sciences 37, 135–162.

Secord, R., Gingerich, P.D., Lohmann, K.C., MacLeod, K.G., 2010. Continental warming preceding the Palaeocene–Eocene thermal maximum. Nature 467, 955–958. http://dx.doi.org/10.1038/nature09441.

Sephton, M.A., Looy, C.V., Veefkind, R.J., Brinkhuis, H., de Leeuw, J.W., Visscher, H., 2002. Synchronous record of $\delta^{13}C$ shifts in the oceans and atmosphere at the end of the Permian. Geological Society of America Special Papers 356, 455–462. http://dx.doi.org/10.1130/0-8137-2356-6.455.

Sepkoski Jr., J.J., 1996. Patterns of Phanerozoic extinction: a perspective from global data bases. In: Walliser, O.H. (Ed.), Global Events and Event Stratigraphy in the Phanerozoic. Springer, Berlin Heidelberg, pp. 35–51.

Shahack-Gross, R., Tchernov, E., Luz, B., 1999. Oxygen isotopic composition of mammalian skeletal phosphate from the Natufian Period, Hayonim Cave, Israel: diagenesis and paleoclimate. Geoarchaeology 14, 1–13. http://dx.doi.org/10.1002/(SICI)1520-6548(199901)14:1<1::AID-GEA1>3.0.CO;2-8.

Shishkin, M.A., Rubidge, B.S., Hancox, P.J., 1995. Vertebrate biozonation of the Upper Beaufort Series of South Africa—a new look on correlation of the Triassic biotic events in Euramerica and southern Gondwana. Proceedings of the Sixth Symposium on Mesozoic Terrestrial Ecosystems and Biota, Beijing, pp. 39–41.

Smith, R.M.H., 1995. Changing fluvial environments across the Permian–Triassic boundary in the Karoo Basin, South Africa and possible causes of tetrapod extinctions. Palaeogeography, Palaeoclimatology, Palaeoecology 117, 81–104. http://dx.doi.org/10.1016/0031-0182(94)00119-S.

Smith, R.M.H., Botha-Brink, J., 2014. Anatomy of a mass extinction: sedimentological and taphonomic evidence for drought-induced die-offs at the Permo-Triassic boundary in the main Karoo Basin, South Africa. Palaeogeography, Palaeoclimatology, Palaeoecology 396, 99–118. http://dx.doi.org/10.1016/j.palaeo.2014.01.002.

Smith, R.M.H., Eriksson, P.G., Botha, W.J., 1993. A review of the stratigraphy and sedimentary environments of the Karoo-aged basins of Southern Africa. Journal of African Earth Sciences (and the Middle East), Geology and Development in Southern Africa 16, 143–169. http://dx.doi.org/10.1016/0899-5362(93)90164-L.

Smith, R.M.H., Ward, P.D., 2001. Pattern of vertebrate extinctions across an event bed at the Permian–Triassic boundary in the Karoo Basin of South Africa. Geology 29, 1147–1150. http://dx.doi.org/10.1130/0091-7613(2001)029<1147:POVEAA>2.0.CO;2.

Smith, R., Rubidge, B., Van der Walt, M., 2012. Therapsid biodiversity patterns and paleoenvironments of the Karoo Basin, South Africa. In: Chinsamy-Turan, A. (Ed.), Forerunners of Mammals: Radiation, Histology, Biology, pp. 31–62 (Indiana University Press, Bloomington).

Sobolev, S.V., Sobolev, A.V., Kuzmin, D.V., Krivolutskaya, N.A., Petrunin, A.G., Arndt, N.T., Radko, V.A., Vasiliev, Y.R., 2011. Linking mantle plumes, large igneous provinces and environmental catastrophes. Nature 477, 312–316. http://dx.doi.org/10.1038/nature10385.

Song, H., Wignall, P.B., Tong, J., Yin, H., 2013. Two pulses of extinction during the Permian–Triassic crisis. Nature Geoscience 6, 52–56. http://dx.doi.org/10.1038/ngeo1649.

Stanley, S.M., Yang, X., 1994. A double mass extinction at the end of the Paleozoic Era. Science 266, 1340–1344. http://dx.doi.org/10.1126/science.266.5189.1340.

Please cite this article as: Rey, K., et al., Global climate perturbations during the Permo-Triassic mass extinctions recorded by continental tetrapods from South Africa, Gondwana Research (2015), http://dx.doi.org/10.1016/j.gr.2015.09.008

Sun, Y., Joachimski, M.M., Wignall, P.B., Yan, C., Chen, Y., Jiang, H., Wang, L., Lai, X., 2012. Lethally hot temperatures during the Early Triassic greenhouse. Science 338, 366–370. http://dx.doi.org/10.1126/science.1224126.

Tarnowski, C.P., Ignelzi, M.A., Morris, M.D., 2002. Mineralization of developing mouse calvaria as revealed by Raman microspectroscopy. Journal of Bone and Mineral Research 17, 1118–1126. http://dx.doi.org/10.1359/jbmr.2002.17.6.1118.

Thackeray, J.F., van der Merwe, N.J., Lee-Thorp, J.A., Sillen, A., Lanham, J.L., Smith, R., Keyser, A., Monteiro, P.M.S., 1990. Changes in carbon isotope ratios in the late Permian recorded in therapsid tooth apatite. Nature 347, 751–753. http://dx.doi.org/10.1038/347751a0.

Tong, J., Yin, H., Zhang, K., 1999. Permian and Triassic Sequence Stratigraphy and Sea Level Changes of Eastern Yangtze Platform. China University of Geosciences, p. 10 (English).

Torsvik, T.H., Van der Voo, R., Preeden, U., Mac Niocaill, C., Steinberger, B., Doubrovine, P.V., van Hinsbergen, D.J., Domeier, M., Gaina, C., Tohver, E., Meert, J.G., McCausland, P.J.A., Cocks, L.R.M., 2012. Phanerozoic polar wander, palaeogeography and dynamics. Earth-Science Reviews 114, 325–368.

Trautz, O.R., 1967. Crystalline mineralization of dental mineral, in: Structural and Chemical Organization of Teeth. Miles AED, San Diego, pp. 165–200.

Trotter, J.A., Williams, I.S., Nicora, A., Mazza, M., Rigo, M., 2015. Long-term cycles of Triassic climate change: a new $\delta^{18}O$ record from conodont apatite. Earth and Planetary Science Letters 415, 165–174. http://dx.doi.org/10.1016/j.epsl.2015.01.038.

Tudge, A.P., 1960. A method of analysis of oxygen isotopes in orthophosphate—its use in the measurement of paleotemperatures. Geochimica et Cosmochimica Acta 18, 81–93. http://dx.doi.org/10.1016/0016-7037(60)90019-3.

van der Walt, M., Day, M., Rubidge, B., Cooper, A.K., Netterberg, I., 2010. A new GIS-based biozone map of the Beaufort Group (Karoo Supergroup), South Africa. Palaeontologica Africana 45, 1–5.

Vennemann, T.W., Hegner, E., Cliff, G., Benz, G.W., 2001. Isotopic composition of recent shark teeth as a proxy for environmental conditions. Geochimica et Cosmochimica Acta 65, 1583–1599. http://dx.doi.org/10.1016/S0016-7037(00)00629-3.

Viglietti, P.A., Smith, R.M.H., Compton, J.S., 2013. Origin and palaeoenvironmental significance of *Lystrosaurus* bonebeds in the earliest Triassic Karoo Basin, South Africa. Palaeogeography, Palaeoclimatology, Palaeoecology 392, 9–21. http://dx.doi.org/10.1016/j.palaeo.2013.08.015.

Voigt, S., Hminna, A., Saber, H., Schneider, J.W., Klein, H., 2010. Tetrapod footprints from the uppermost level of the Permian Ikakern Formation (Argana Basin, Western High Atlas, Morocco). Journal of African Earth Sciences 57, 470–478. http://dx.doi.org/10.1016/j.jafrearsci.2009.12.003.

Ward, P.D., Botha, J., Buick, R., Kock, M.O.D., Erwin, D.H., Garrison, G.H., Kirschvink, J.L., Smith, R., 2005. Abrupt and gradual extinction among Late Permian land vertebrates in the Karoo Basin, South Africa. Science 307, 709–714. http://dx.doi.org/10.1126/science.1107068.

Weidlich, O., 2002. Permian reefs re-examined: extrinsic control mechanisms of gradual and abrupt changes during 40 my of reef evolution. Geobios 35 (Supplement 1), 287–294. http://dx.doi.org/10.1016/S0016-6995(02)00066-9.

Wignall, P.B., Sun, Y., Bond, D.P.G., Izon, G., Newton, R.J., Védrine, S., Widdowson, M., Ali, J.R., Lai, X., Jiang, H., Cope, H., Bottrell, S.H., 2009. Volcanism, mass extinction, and carbon isotope fluctuations in the Middle Permian of China. Science 324, 1179–1182. http://dx.doi.org/10.1126/science.1171956.

Yang, X., Shi, G., Liu, J., Chen, Y., Zhou, J., 2000. Inter-taxa differences in extinction process of Maokouan (Middle Permian) fusulinaceans. Science in China Series D: Earth Sciences 43, 633–637. http://dx.doi.org/10.1007/BF02879507.

Yue, W., Yugan, J., 2000. Permian palaeogeographic evolution of the Jiangnan Basin, South China. Palaeogeography, Palaeoclimatology, Palaeoecology 160, 35–44. http://dx.doi.org/10.1016/S0031-0182(00)00043-2.

Zazzo, A., Lécuyer, C., Mariotti, A., 2004a. Experimentally-controlled carbon and oxygen isotope exchange between bioapatites and water under inorganic and microbially-mediated conditions. Geochimica et Cosmochimica Acta 68, 1–12. http://dx.doi.org/10.1016/S0016-7037(03)00278-3.

Zazzo, A., Lécuyer, C., Sheppard, S.M.F., Grandjean, P., Mariotti, A., 2004b. Diagenesis and the reconstruction of paleoenvironments: a method to restore original $\delta^{18}O$ values of carbonate and phosphate from fossil tooth enamel. Geochimica et Cosmochimica Acta 68, 2245–2258. http://dx.doi.org/10.1016/j.gca.2003.11.009.

Zhong, Y.-T., He, B., Mundil, R., Xu, Y.-G., 2014. CA-TIMS zircon U–Pb dating of felsic ignimbrite from the Binchuan section: implications for the termination age of Emeishan large igneous province. Lithos, Special Issue Permian large igneous provinces: Characteristics, mineralization and paleo-environment effects 204 pp. 14–19. http://dx.doi.org/10.1016/j.lithos.2014.03.005.

Zhou, M.-F., Malpas, J., Song, X.-Y., Robinson, P.T., Sun, M., Kennedy, A.K., Lesher, C.M., Keays, R.R., 2002. A temporal link between the Emeishan large igneous province (SW China) and the end-Guadalupian mass extinction. Earth and Planetary Science Letters 196, 113–122. http://dx.doi.org/10.1016/S0012-821X(01)00608-2.

Please cite this article as: Rey, K., et al., Global climate perturbations during the Permo-Triassic mass extinctions recorded by continental tetrapods from South Africa, Gondwana Research (2015), http://dx.doi.org/10.1016/j.gr.2015.09.008